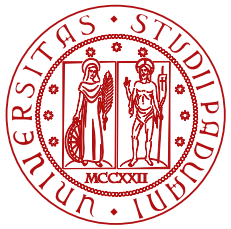

UNIVERSITÀ DEGLI STUDI DI PADOVA

DEPARTMENT OF GEOSCIENCES

MASTER THESIS

Ground Thermal Properties By Neural Networks on Well-log datasets

AUTHOR

Mahdi Pabakhsh

Student ID 2039875

Master of Geophysics for Natural Risks and Resources

PROFESSOR

Prof. Antonio Galgaro

University of Padova

ACADEMIC YEAR
JULY 2024

To my family
and friends

Abstract

This research focuses on using well-log data from abandoned oil and gas wells to predict ground thermal properties and assess geothermal potential. The study utilizes an Artificial Neural Network (ANN) approach to predict thermal conductivity in three oil fields. Initially, thermal conductivity is calculated using recommended values for each mineral from the UNIPD Cheap-GSHPs thermal database and a geometric average (Clauser, 2006) in the first oil field. It is then validated by laboratory measurements, showing a strong correlation. The ANN model incorporates seven training datasets, including Gamma Ray (GR), Neutron Porosity (NPHI), Sonic Travel Time (DT), Bulk Density (RHOB), Total Porosity (PHIT), and Resistivity logs, with thermal conductivity as the associated log. The model is trained in the first oil field and validated, achieving a correlation coefficient of over 95%. Performance metrics (MAE, MSE, and R-squared) for thermal conductivity predictions are reported for all oil fields. The study also explores the relationship between predicted thermal conductivity and other properties, such as porosity and density. The study identified three oil fields with different properties for geothermal applications. The first oil field, with a thermal conductivity of about 2.7 $W/m \cdot K$ and a temperature of 115°C, is suitable for medium geothermal purposes. The second oil field, made up of limestone, has a thermal conductivity of 2.8 $W/m \cdot K$ and a temperature of138°C, making it ideal for high geothermal applications. The third oil field, composed of dolomite, exhibits thermal conductivity ranging between 2.9 $W/m \cdot K$ and 3.0 $W/m \cdot K$ and temperatures between 85°C and 105°C, making it suitable for shallow geothermal purposes

Contents

List of Figures

1

Introduction

Geothermal energy, often overlooked in discussions about renewable energy, holds immense potential for meeting the increasing energy demands of emerging countries and facilitating energy transition worldwide. Unlike other renewable sources, geothermal energy offers a consistent and nearly limitless heat supply from the Earth's interior. However, unlocking this potential presents various challenges, particularly in effectively characterizing and utilizing geothermal resources.

Deep geothermal reservoirs, nestled within highly heterogeneous geological formations, pose unique challenges for exploration and development. Overcoming these challenges requires interdisciplinary methodologies encompassing volcanology, geophysics, geochemistry, and geothermal sciences. Additionally, improving assessment methods for geothermal systems, including high-temperature borehole thermal energy storage (HT-BTES) and direct heating applications, is essential for maximizing their utilization.

Despite these challenges, geothermal energy, both deep and near-surface, offers promising solutions for addressing energy needs sustainably. While large-scale geothermal installations face hurdles such as high investment costs and societal acceptance, smaller-scale applications offer a viable pathway to reducing energy consumption and carbon emissions, especially in household heating. Furthermore, advancements in technology, such as heat pumps and enhanced geothermal systems (EGS), are driving rapid growth in both the electricity and heat sectors of the geothermal industry [17].

In this thesis, we delve into the utilization of geothermal energy by analyzing ground thermal properties estimation. We will focus on applying neural networks to study well-log datasets. Through the power of machine learning, our aim is to improve our understanding of ground thermal characteristics and contribute to the sustainable development of geothermal resources. This research aims to address key challenges in geothermal energy exploration and promote its integration into the global energy landscape.

1.1 Ways of heat transport

Geothermal heat is not straightforward. It involves depth, temperature gradients, and geological formations. There are two categories: deep and near-surface geothermal

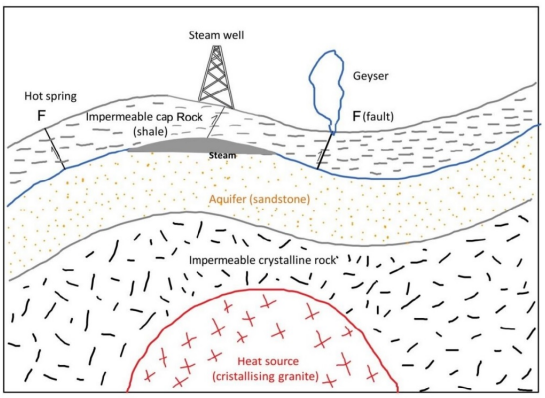

Figure 1.1: Schematic section showing the main components of a geothermal system. [5]

energy, separated at around 400 meters. Deep geothermal energy is at greater depths. Geothermal energy near the surface is accessible without excavating beyond 400 meters.

1.1.1 Convection

Convection is the primary heat transport mechanism within the Earth's interior. It facilitates material movement through hot, deformable solids by temperature differentials between the Earth's surface and interior, resulting in a circulation pattern. Convective heat transport is efficient and results in minor temperature fluctuations across the convecting layer's depth. Convective heat flow occurs when liquids or gases mobilize, carrying their heat along with them.

1.1.2 Conduction

The Earth's crust is a rigid, brittle layer made up of fragmented lithospheric plates that interact and move across the Earth's surface due to underlying convective forces. Heat transfer in the top 100 kilometers of the crust occurs mainly through conduction.

1.1.3 Radiation

Radiation transmits heat from the Sun and is significant for shallow geothermal energy. Past 20 meters in depth, solar radiation diminishes, and temperature regulation relies on geothermal heat flow. This type of heat transfer involves electromagnetic radiation without mass exchange or dependence on a transmission medium.

1.2 GEOTHERMAL SYSTEMS

1.2.1 Conventional geothermal systems

The most commonly exploited geothermal resources rely on the presence of water circulating through the rock to extract heat and convey it to the surface. Within these systems, several essential elements are consistently present.

Reservoir

Figure 1.2: Manifestations of geothermal activity (geysers) in different geothermal fields. The left picture was taken in New Zealand and the right picture is of Iceland. [5]

Geothermal reservoir rocks have porosity and permeability, which store water and facilitate fluid flow. Favorable reservoirs include sandstones and limestone formations. Fracture-induced permeability creates secondary pathways that connect pores and facilitate fluid migration[5].

Geothermal aquifers can be unconfined or confined. Unconfined aquifers are recharged by rainfall, while confined aquifers lie beneath a cap rock and do not receive direct recharge from rainfall. As a result, confined aquifers can have high fluid pressure.

Cap rock

The cap rock is a crucial seal for geothermal aquifers. It is made up of impermeable materials such as shales, clays, evaporites, or unfractured lavas. It prevents geothermal fluid from escaping upward, enhancing the efficiency of geothermal exploitation in the area.

Permeable structures

Faults in the cap rock act as pathways for escaping steam and hot water, creating geothermal manifestations. These include fumaroles, geysers, and hot springs. These visible phenomena offer evidence of subsurface heat and fluid movement.

Heat source

Geothermal systems have varying heat sources depending on the region. In high-enthalpy areas with frequent volcanic activity, the primary source is a cooling or solidifying magma. In low-enthalpy regions, the heat source may be in deep sedimentary basins with warm water from the geothermal gradient. Alternatively, hot dry rocks with high natural heat production can be a source, though fluid circulation is difficult due to low permeability[5].

To extract geothermal energy, artificial fractures are created in the rock using stimulation techniques. These fractures enhance permeability and allow fluid circulation.

1.3 Unconventional geothermal systems

Geothermal systems often lack key elements, prompting the use of advanced technologies for economic exploitation. Additional stimulation techniques such as hydraulic, chemical or thermal methods may be needed to enhance permeability in unproductive wells[5].

According to the Iceland Survey, the main types of unconventional geothermal systems are as follows:

1.3.1 Hot-Dry Rock Systems (HDR)

Heat is stored in low-permeability rock formations, like shallow granite bodies. Reservoirs are stimulated to create necessary permeability for well performance. Water is injected to extract heat, ideally producing steam. Examples are Fenton Hill (US) and Cornwall (UK)[5].

1.3.2 Enhanced Geothermal Systems (EGS)

Hydraulic fracturing, or "fracking," establishes artificial permeability and enables fluid circulation for heat transfer. This involves injecting water, sand, and chemicals at high pressure to create and expand fractures. Examples include Soultz (France) and Cooper Basin (Australia)[5].

1.3.3 Supercritical Geothermal Systems (SGS)

Fluids in these systems undergo high temperatures and pressure in reservoirs. At the borehole, the fluid exhibits properties of superheated steam, making it difficult to differentiate between liquid and vapor phases. Examples include IDDP (Iceland) and Geysers (USA)[5].

1.4 study of geothermal properties

Geothermal energy potential is assessed with a multidisciplinary approach using scientific and technological methods. Here are the key steps involved:

Geological Mapping

Geothermal energy surveys target regions with tectonic plate boundaries, volcanic activity, and high heat flow.

Geophysical Surveys

Geophysical surveys can identify underground structures and potential hot water or steam reservoirs.

Geochemical Analysis

Geochemical surveys detect geothermal fluids by analyzing water, soil gases, and rocks for chemical signatures.

Temperature Measurements

Direct temperature measurements are collected at the surface and in boreholes to assess subsurface thermal gradients and identify areas of high temperature[5].

Remote Sensing

Using satellite imagery and aerial surveys can identify surface features such as hot springs, fumaroles, and altered surface geology, which can indicate geothermal activity.

Hydrological Analysis

The distribution and characteristics of surface water bodies, such as hot springs and thermal features, provide insight into subsurface heat sources and fluid flow pathways.

Numerical Modeling

Geological data predicts geothermal potential.

Exploratory Drilling

Exploratory drilling is conducted to confirm the presence and characteristics of geothermal resources identified through other methods. This involves drilling test wells to measure temperatures, assess fluid chemistry, and determine reservoir properties.

1.5 Petrophysical properties of geothermal

Several key factors are considered when studying geothermal properties, with some being more important depending on the context. Here are some of the most crucial properties

Temperature

Perhaps the most important property is that it directly influences the feasibility and efficiency of geothermal energy extraction. Understanding temperature gradients and variations in the subsurface is essential for assessing the potential of a geothermal resource.

Theraml Conductivity

Thermal conductivity measures a rock's ability to conduct heat. In geothermal systems, rocks with higher thermal conductivity transfer heat more efficiently, which helps to extract thermal energy from the reservoir. It's important to understand the thermal conductivity of subsurface formations to evaluate the heat transfer dynamics within a geothermal reservoir.

Permeability

The permeability of subsurface rocks is crucial for efficient geothermal fluid circulation and productivity.

Porosity

The volume of pore space in rocks determines their capacity to store geothermal fluids. Rocks with higher porosity can hold more fluid, increasing the potential energy yield of a geothermal reservoir.

Rock Type

Rock types have different thermal conductivities, impacting heat transfer efficiency in the subsurface. Knowing the thermal properties of formations helps assess geothermal heat extraction potential.

Fluid Chemistry

Geothermal fluid composition affects the system's corrosiveness and scaling potential. Monitoring fluid chemistry optimizes energy production and reduces equipment corrosion.

Reservoir Depth

The depth of a geothermal reservoir affects drilling costs, resource access, and heat extraction efficiency. Deeper reservoirs may have higher temps but require costlier drilling.

Fracture Network

Fractures and faults increase permeability, allowing fluid flow and heating in geothermal reservoirs.

Rock Density

Rock density affects a rock formation's thermal and mechanical properties. Denser rocks have higher thermal conductivity and heat storage capacity, impacting heat exchange efficiency in geothermal reservoirs.

Fluid content

Fluid content affects a geothermal reservoir's heat extraction potential. Rocks with more fluid store more thermal energy and facilitate heat transfer. Steam has a higher heat capacity than liquid water, making it more energy efficient.

Geoscientists and engineers use petrophysical techniques to understand fluid content in geothermal reservoirs. They can optimize reservoir management strategies and enhance geothermal energy project performance by quantifying fluid content.

Specific Heat Capacity

The specific heat capacity of a substance is the amount of heat required to increase its temperature by one degree Celsius. In geothermal systems, this capacity affects how much thermal energy can be stored in the rock and fluid phases, which impacts the overall heat exchange processes and reservoir behavior.

1.6 Considerations of Risk and Cost

When studying geothermal properties, it's important to consider the risks and costs of different methods. Here's how these factors can influence the selection of study methods[9].

Risk Assessment

- Exploratory Drilling: While exploratory drilling directly measures geothermal properties, it is also one of the riskiest and most expensive methods. There's a significant chance of encountering unexpected subsurface conditions or failing to find viable geothermal resources, leading to high exploration costs and potential financial losses[9].
- Geophysical Surveys: Geophysical methods such as seismic and magnetotelluric surveys carry lower risks than drilling, as they provide indirect measurements of subsurface properties. However, there's still a risk of misinterpretation or ambiguity in the survey data, which could lead to inaccurate assessments of geothermal potential[9].
- Remote Sensing and Satellite Imagery: emote sensing techniques offer a non-invasive way to identify surface features associated with geothermal activity, such as hot springs and altered surface geology. While these methods carry minimal direct risks, there's a risk of false positives or misinterpretation of surface signals, leading to potential misallocation of resources [9].
- Sample collection for laboratory analysis is less risky than drilling or geophysical surveys. However, contamination or alteration during collection, handling, and transport can impact accuracy[9].
- Various laboratory techniques, such as core analysis, petrography, XRD, and fluid analysis, provide detailed information on geothermal reservoirs. These methods are generally safe, but there is a risk of experimental errors that could impact reliability[9].

Cost Considerations

- Exploratory Drilling: Exploratory drilling is costly due to the high drilling rigs, equipment, and personnel expenses. Unexpected challenges or greater depths can also increase costs[9].

- Geophysical Surveys: Geophysical surveys are cheaper than drilling, but costs vary based on factors like location complexity, equipment, and required expertise. Larger surveys or more advanced techniques can be more expensive[9].
- Remote Sensing and Satellite Imagery: Remote sensing techniques are frequently the less expensive and more effective choice for the initial exploration and evaluation of geothermal potential on a regional scale. The costs of remote sensing are significantly lower in comparison to drilling or extensive geophysical surveys, making it a valuable tool for the preliminary screening of potential geothermal sites[9].
- Sample Collection: The cost of acquiring rock and fluid samples for laboratory analysis is relatively low compared to drilling or extensive geophysical surveys. However, the costs can vary based on sample location, accessibility, transportation, and storage requirements[9].
- Analysis techniques may incur various costs, such as equipment, personnel, sample preparation, testing, and interpretation of results, depending on the complexity and scope of the analysis[9]

.

1.7 Repurposing Abandoned Oil and Gas Wells for Sustainable Energy Development

Repurposing abandoned oil and gas wells for geothermal energy production offers numerous benefits[30].

Cost Savings

Utilizing existing wells can reduce upfront costs for geothermal projects. These wells have already incurred permitting, site preparation, and drilling operations expenses, resulting in overall cost savings[30].

Time Efficiency

Geothermal operators can save time and accelerate project timelines by using abandoned oil and gas wells to access the subsurface to explore and develop geothermal resources[30].

Access to Data

Abandoned wells often come with valuable geological and engineering data, including well logs, core samples, and historical production records. This information provides insights into subsurface formations, reservoir characteristics, and fluid properties, facilitating informed decision-making and optimizing geothermal operations[30].

Infrastructure Reuse

Repurposing existing wells reduces environmental disturbance and simplifies project logistics, leading to more efficient resource utilization[30].

Environmental Benefits

Geothermal projects can reuse abandoned oil and gas wells, minimizing the environmental impact of new well drilling and aligning with sustainability goals[30].

Risk Mitigation

Abandoned wells have already undergone drilling and completion processes, reducing the uncertainties and risks typically associated with new well construction. This

enhances project predictability and helps mitigate potential drilling-related challenges and setbacks[30].

Existing Infrastructure

Abandoned oil and gas wells have pre-existing infrastructure, including wellheads, casing, and surface facilities, which can be repurposed for geothermal operations. This infrastructure is a significant investment that can reduce the overall costs of geothermal projects. Rather than constructing new infrastructure, geothermal operators can refurbish and retrofit existing components, saving both time and money[30].

Subsurface Access

Exploring geothermal energy through drilling new wells can be a risky and unpredictable process due to geological complexity, drilling hazards, and unknown subsurface conditions. However, abandoned oil and gas wells offer reliable access to the subsurface and potential geothermal reservoirs. Using existing wellbores allows geothermal companies to avoid uncertainties and risks associated with new well drilling, resulting in more predictable project outcomes[30].

Geological Information

Abandoned wells are a valuable source of geological data, including well logs, core samples, and geophysical surveys. This information can provide important insights into subsurface formations, rock properties, and fluid characteristics, which are essential for assessing the geothermal potential of a site. Geothermal operators can better understand the geological setting by analyzing this data, identifying favorable reservoir conditions, and optimizing drilling and production strategies[30].

Regulatory Considerations

Repurposing abandoned wells for geothermal purposes can provide regulatory benefits compared to drilling new wells. In several jurisdictions, regulatory requirements for re-entering and repurposing existing wells are less strict than those for drilling new wells. This simplified regulatory process can expedite project permitting and approvals, reducing administrative burdens and accelerating project timelines[30].

Repurposing abandoned oil and gas wells for geothermal energy offers a cost-effective, time-efficient, and environmentally sustainable approach to accessing subsurface resources. Using existing infrastructure and data, geothermal operators can expedite project development and optimize resource utilization, thereby contributing to the growth and sustainability of the geothermal energy industry[30].

1.8 Optimizing geothermal exploration with well-log data and neural networks

I conducted a thorough study using well-log data from multiple wells to analyze important petrophysical properties required for geothermal exploration. Our primary objective was to determine key parameters such as the formation's porosity, fluid content, and lithology. We utilized advanced machine learning techniques, including neural networks, to develop predictive models that estimate the thermal conductivity of each composition of the formation.

By using existing well-log data and advanced computational techniques, we were

able to save both time and money in studying the physical properties of geothermal sources. Our approach also minimized risks involved in traditional methods, such as exploratory drilling, by providing precise predictions without needing extensive field-work or intrusive sampling. This innovative approach improves geothermal resource assessment and optimizes renewable exploration.

2

Review of Literature on Ground Thermal Properties

2.1 Ground Thermal Properties for GSHP Applications

The study conducted by Antonio Galgaroa et al(2020). presents an updated database of ground thermal properties, which was developed as part of the EU-funded Cheap-GSHPs project. This project aims to support the design of Ground Source Heat Exchanger (GSHP) systems. Ground thermal properties are vital in GSHP system design, as climate, building characteristics, and ground conditions influence them. One of the biggest challenges in GSHP system design is accurately evaluating thermal properties because undersized or oversized bore fields can significantly impact system efficiency and costs. The Cheap-GSHPs project addresses this challenge by developing a Decision Support System (DSS) and a comprehensive database that provides thermal conductivity values for rocks and sediments, which are crucial for system design. Methods for determining thermal properties include in-situ tests like Thermal Response Tests (TRT) and laboratory measurements. Overall, the accurate assessment of ground thermal properties is essential for designing efficient and cost-effective GSHP systems, and the resources developed by the Cheap-GSHPs project facilitate informed decision-making in GSHP system design and implementation[7].

According to Sarbu and Sebarchievici's 2014 study, low-enthalpy geothermal energy is a widely used renewable energy source for heating and cooling buildings. This method involves closed-loop geothermal systems that use borehole heat exchangers to transfer heat between the ground and the building through a fluid. When designing such systems, the authors suggest considering various factors such as climate, building characteristics, and ground conditions[7].

The "Cheap-GSHPs" project was initiated in June 2015 and concluded in May 2019 under the Horizon 2020 EU framework program for Research and Innovation. Partners from nine European countries led the project to reduce engineering and installation costs for closed-loop geothermal systems. To achieve this goal, the project developed a Decision Support System (DSS) to assist in system design, as described in Carnieletto et al.'s 2019 study[7].

The DSS is a user-friendly web-based application that integrates climate data, build-

ing requirements, and geological information to help users select appropriate components for new GSHP systems, as De Carli et al. explained in 2018. Additionally, the project developed a thermal properties database to evaluate the local thermal exchange potential, as outlined by Müller et al. in 2018. This enhanced database was further developed during the EU project GEO4CIVHIC to support the design of geothermal systems for new constructions and retrofitting historical buildings[7].

As the reference data for thermal conductivity, the UNIPD Cheap-GSHPs thermal database is used in this case study.

2.2 Factors that Affect Ground Thermal Properties.

The significance of thermal conductivity (TC) for calculating heat flow in geothermal studies is highlighted by the research conducted by Popov et al. (1999) and Lide (1998). Various laboratory methods such as Divided-bar, Line-source, and Optical scanning are used to measure TC, which is influenced by intrinsic and extrinsic factors explained by Jumikis (1966), Harmathy (1970), and others. TC determination methods include empirical relationships (Özkahraman et al., 2004; El Sayed, 2011; Duchkov et al., 2014), well log data analysis (Demongodin et al., 1991; Hartmann et al., 2005, 2008), and the application of artificial intelligence (Goutorbe et al., 2006; Singh et al., 2007; Vaferi et al., 2014; Gitifar et al., 2014). The relationships between TC and petrophysical properties are studied in various rock types, including sandstone (El Sayed, 2011; Haffen et al., 2013; Esteban et al., 2015) and carbonates (Kazatchenko et al., 2006). Gupta and Sharma (2012) investigated correlations in quartzite rocks, while Hrouda and Kapika (1986) and Vishnu et al. (2010) explored magnetic susceptibility effects. Benayad et al. (2013, 2014) and Aïfa et al. (2014) studied the Hamra Quartzites reservoir. In this study, the application of Radial Basis Function (RBF) neural networks in geothermics is proposed to efficiently predict TC, particularly in fractured samples, and investigate relationships between TC, porosity, density, and permeability in the Hamra Quartzites reservoir[34].

Ahmed Ali Zerrouki et al(2019). studied the relationship between thermal conductivity (TC) and petrophysical parameters in the Hamra Quartzites reservoir, which is important for rock heat flow calculations. They proposed estimating TC through linear and nonlinear relationships based on parameters such as mineralogy and porosity. Porosity, density, and permeability were measured to predict TC. The study found a moderate correlation between TC and porosity and a weak correlation between TC and density and permeability. Radial Basis Function (RBF) neural networks were used to achieve precise TC prediction, which correlated closely with laboratory measurements[34].

2.2.1 Porosity

Porosity refers to the empty space within a rock or soil sample. Generally, the higher the porosity, the lower the thermal conductivity because empty spaces act as insulators, impeding heat transfer. However, the relationship between porosity and thermal conductivity can vary depending on the type of empty spaces present, such as connected or isolated pores, and the fluid content within those spaces. For instance,

in dry rocks, increased porosity often results in lower thermal conductivity due to the presence of air-filled gaps, which are poor conductors of heat. On the other hand, in water-saturated rocks, higher porosity can lead to higher thermal conductivity because water is a better conductor of heat than air[1].

2.2.2 Density

Density is a measure of the amount of mass that is present per unit volume of a particular material. Denser materials tend to have higher thermal conductivity (TC) because the atoms or molecules within them are packed more closely together. This allows for more efficient heat transfer through the atomic or molecular vibrations. Rocks with higher mineral densities, such as those rich in quartz or feldspar, typically exhibit higher thermal conductivity compared to less dense rocks like those made up of shale or clay-rich formations[1].

2.2.3 Permeability

Permeability refers to the property of a material to allow fluids to pass through. Although permeability does not directly impact thermal conductivity, it can indirectly influence fluid flow within the rock matrix. In porous materials, fluid movement can enhance heat transfer by transporting heat away from hotter regions or toward cooler regions. On the other hand, low permeability can limit fluid flow and hinder convective heat transfer, leading to a lower overall thermal conductivity[1].

2.2.4 Fluid Content

The type and distribution of fluids present in the pore spaces can significantly influence the thermal conductivity (TC) of rocks. When rocks are saturated with water, for example, they exhibit higher TC than those that are dry or filled with gas due to water's higher thermal conductivity [1].

In addition to the fluid type, the degree of saturation also plays a role in TC. As the volume fraction of fluid in the pore space increases, so does TC because the fluid facilitates heat transfer through the rock matrix.

Another factor affecting TC is the spatial distribution of fluids within the rock pores. Rocks with interconnected pores filled with fluids tend to have higher TC than those with isolated pockets of fluid, as the former allows for more efficient heat transfer.

Finally, phase changes of fluids within the rock matrix, such as evaporation, condensation, or the transition between liquid and gas, can also impact TC by altering the fluid's thermal properties and its heat transfer capabilities within the rock[1].

2.2.5 Mineral composition of rock

The ability of rocks to conduct heat is influenced by their composition, a property referred to as thermal conductivity (TC). Various minerals possess different abilities to conduct heat, and the type and quantity of minerals in a rock determine its TC. The following are some ways in which mineral composition affects TC:

- Certain minerals: such as quartz, feldspar, and mica, are excellent heat conductors, whereas others, such as clay minerals, are not. Rocks that have a higher proportion of high-conductivity minerals have higher TC.
- Mineral Quantity: The number of minerals in a rock can impact its TC. A rock with a higher concentration of quartz or feldspar will have greater TC than one composed mainly of clay minerals.
- Mineral grain size: The size of minerals in a rock can also affect TC. Rocks with smaller grains conduct heat more effectively because they provide more pathways for heat transfer. Fine-grained textured rocks generally have higher TC than coarse-grained ones.
- Mineral bonding: How minerals bond in a rock can also impact TC. Rocks with tightly bonded minerals conduct heat better than those with loosely bonded minerals. Strong bonds facilitate the movement of heat from one mineral to another.
- Anisotropy: Some minerals conduct heat differently in different directions. Rocks with these minerals can have varying TC in different rock parts, depending on how the minerals are arranged.

[1].

2.2.6 Temperature

Temperature is a crucial factor that influences rocks' thermal conductivity (TC). Let's explore how temperature affects TC:

- Temperature Dependence: Thermal conductivity often depends on temperature, which can vary with temperature changes. Generally, the TC of most rocks tends to increase with temperature. Higher temperatures lead to greater atomic or molecular vibrations within the rock matrix, which enhances heat transfer.
- Thermal Expansion: As temperature increases, materials usually expand, affecting the packing of mineral grains within the rock matrix. Changes in mineral packing can affect the pathways available for heat conduction, thereby impacting TC.
- Phase Transitions: Temperature changes may also cause phase transitions within the rock, such as melting or crystallizing minerals. These phase transitions can alter the thermal properties of the rock and affect its TC.
- Hydrothermal Effects: In geothermal systems, temperature gradients within the subsurface can drive fluid flow and alter rocks' mineralogy and pore structure through hydrothermal alteration. These changes can significantly impact TC and heat transfer processes in geothermal reservoirs.
- In situ Conditions: The TC of rocks under in situ conditions, where they experience the subsurface environment's actual temperature and pressure conditions, may differ from laboratory measurements conducted at ambient conditions. Therefore, it's essential to consider the temperature regime of the geothermal reservoir when interpreting TC data.

[1].

2.3 Neural Network Introduction

Neural networks are a fundamental concept in machine learning and artificial intelligence, inspired by the structure and function of the human brain. They are a class of algorithms designed to recognize patterns and learn from data. The basic principle

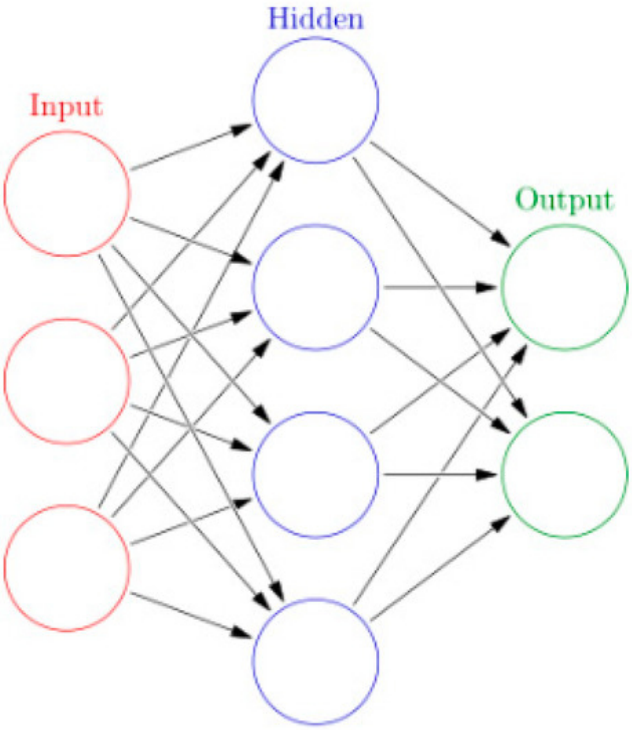

Figure 2.1: Artificial neural network [13]

of a neural network involves processing input data through a series of interconnected layers of artificial neurons, or nodes, to produce an output. The architecture of a neural network typically consists of three main types of layers figure2.1:

- Input Layer: This layer receives the initial input data and passes it to the next layer for processing. Each neuron in this layer represents a feature or attribute of the input data.[33]
- Hidden Layers: The actual computation and learning occur in these layers. Each neuron in a hidden layer receives inputs from the previous layer, applies a transformation (using weights and activation functions), and passes the result to the next layer. Deep neural networks have multiple hidden layers, allowing for complex feature representations and learning of intricate patterns in the data.[33]
- Output Layer: The final layer of the network produces the output based on the processed information from the hidden layers. The number of neurons in the output layer depends on the nature of the taskclassification tasks may have neurons representing different classes. In contrast, regression tasks may have a single neuron for continuous output[33].

The connections between neurons in adjacent layers are characterized by weights, which determine the strength of the connection. During training, these weights are adjusted iteratively through a process called backpropagation, where the network learns to minimize the difference between its predicted output and the actual output using an optimization algorithm like gradient descent[33].

2.3.1 Artificial Neural Network Applications

Neural networks are a powerful tool for data analysis and can learn complex patterns from data to make predictions or classifications. They have many applications, such as[10]:

- Image Recognition and Computer Vision: Convolutional Neural Networks (CNNs) excel in image classification, object detection, and facial recognition tasks. They are commonly used in autonomous vehicles, medical imaging, surveillance systems, and photo-tagging applications.
- Natural Language Processing (NLP): Recurrent Neural Networks (RNNs) and their variants, such as Long Short-Term Memory (LSTM) networks and Transformer models, are used for tasks like sentiment analysis, language translation, text generation, and speech recognition. NLP models power virtual assistants, chatbots, language translation services, and text summarization tools.
- Healthcare: Neural networks are used in medical diagnosis, disease prediction, and personalized treatment recommendations. They analyze medical images (e.g., X-rays and MRI scans) to detect anomalies and assist in drug discovery and genomics research.
- Finance: Neural networks are used in financial forecasting, fraud detection, algorithmic trading, and risk assessment. They analyze market trends, predict stock prices, detect fraudulent transactions, and optimize trading strategies[10].
- Recommendation Systems: Neural networks power recommendation engines in e-commerce, streaming services, and social media platforms. They analyze user behavior and preferences to suggest relevant products, movies, music, or content[10].
- Autonomous Vehicles: Neural networks play a crucial role in self-driving cars for tasks like object detection, lane detection, traffic sign recognition, and decision-making based on sensor inputs. They enable vehicles to perceive and navigate the surrounding environment.
- Manufacturing and Industry 4.0: Neural networks are used for predictive maintenance, quality control, and optimization in manufacturing processes. They analyze sensor data to detect equipment failures, optimize production schedules, and improve product quality.
- Gaming and Entertainment: Neural networks are employed in game development for character animation, behavior prediction, and adaptive gameplay. They also contribute to content creation in the entertainment industry, such as generating music, art, and virtual environments[10].
- Energy and Utilities: Neural networks are used for energy load forecasting, smart grid optimization, and predictive maintenance of energy infrastructure. They help utility companies improve efficiency, reduce downtime, and optimize energy distribution[10].
- Agriculture: Neural networks are applied in precision agriculture for crop monitoring, yield prediction, and pest detection. They analyze satellite imagery, weather data, and soil characteristics to optimize farming practices and maximize crop yield[10].

Artificial Neural Networks (ANN) is a new technology with various applications, such as pattern recognition, prediction, system identification, and control. The ANN is a radial basis function back-propagation network, which means that it can predict the parameters of an experimental system. Its parallel structure and fast learning capacity make it an ideal tool for data analysis. The network uses experimental data such as speed, load, and pressure distribution values for training and testing. It is a feed-forward three-layered network that uses the quick propagation algorithm to update its weight during training. The ANN has a superior performance and can achieve the desired results of the system, making it an excellent tool for analyzing system parameters in practical applications. Artificial Neural Networks (ANN) is a new technology with

various applications, such as pattern recognition, prediction, system identification, and control. The ANN is a radial basis function back-propagation network, which means that it can predict the parameters of an experimental system. Its parallel structure and fast learning capacity make it an ideal tool for data analysis. The network uses experimental data such as speed, load, and pressure distribution values for training and testing. It is a feed-forward three-layered network that uses the quick propagation algorithm to update its weight during training. The ANN has a superior performance and can achieve the desired results of the system, making it an excellent tool for analyzing system parameters in practical applications[10].

2.4 An overview of neural networks in geosciences

Using probabilistic neural networks to classify mineral deposits based on mineralogy and broad rock types was explored by Singer and Kouda (1997). In their study, geoscience information from large mineral databases was integrated to classify deposits based on geoscience information. Their study examined whether a probabilistic neural network could accurately classify deposits by analyzing ore and alteration mineralogy and six generalized rock types[27].

Probabilistic neural networks can provide reliable confidence measures and handle multimodal distributions with Parzen density estimation and Bayes theorem. In their study, a Gaussian kernel weighted each class and variable separately.

A total of 28 well-typed deposits comprised of ore and alteration mineralogy were considered for training, and six types of rock were used. Based on 1005 deposits, 58 minerals were reported, and six rock types were reported based on a restriction to minerals in at least 50% of one deposit type.

Two independent tests were conducted based on a training set that contained 2751 Nevada deposits. A comparison between neural networks' classification and expert classifications showed 53% agreement. While the neural network cannot identify specific deposit types, it does perform well at generalizing. It can identify more than 98% of sites correctly[27].

Among their study's findings is the potential use of probabilistic neural networks to integrate geoscience information and classify deposits by identifying characteristics of the terranes that are conducive to certain deposits[27]. Barton (1986) estimated the frequency of minerals in different types of deposits, which served as the basis for McCammon's (1992) attempt to classify deposits using a combination of estimated mineral frequencies and other geological factors with Prospector II. McCammon managed to classify Alaskan deposits with an 83% success rate. Expert systems like Prospector II rely on human expert knowledge and qualitative principles perceived by experts. However, they face challenges due to internal inconsistencies or dependence on inconsistent information.

On the other hand, inductive learning systems, such as decision trees, artificial neural networks, and statistical pattern recognition, can use pre-classified samples for training and excel in generalization. Singer and Kouda (1997) demonstrated the potential of probabilistic neural networks by correctly classifying 98% of 267 mineral deposits

into eight types based on mineralogy and rock types. They proposed further testing the network's ability to classify deposits based on a simplified representation of mineralogy and six broad rock types. Their study discussed the sources of data and the implementation of probabilistic neural networks. It tested the network's classification accuracy using a large database of expert-typed deposits and comparisons with expert-delineated permissive tracts in Nevada. Finally, they examined classification errors and potential improvements[27].

Anochi, Torres, and Velho (2020) presented two strategies for automatically configuring neural networks using optimization techniques. They tackled a problem of minimizing a single objective using the Multiparticle Collision Algorithm (MPCA) and a problem of minimizing multiple objectives using the Non-Dominated Sorting Genetic Algorithm (NSGA-II). These methods were tested in two geoscience applications: data assimilation for wave evolution equations and mesoscale seasonal climate prediction for precipitation. Their research revealed that automatic network configuration produced better results than the networks defined by experts in both applications. Specifically, in the case of data assimilation and predicting seasonal precipitation for climate, automatic configuration demonstrated superior performance compared to expert-defined networks. The NSGA-II algorithm showed better results in the experiments conducted[2].

Artificial neural networks (ANNs) play an important role in artificial intelligence. Generally speaking, they are characterized as a machine learning framework which has been successfully applied to various applications. The neural networks are inspired by research into the functioning of the neural structure of intelligent organisms, which demonstrates that knowledge is acquired through experience. The artificial neural network (ANN) is a highly efficient machine that can provide robust solutions to problems involving pattern recognition, classification, prediction, optimization, and function approximation. In the field of intelligent control and image processing, neural networks have been applied to solve real-world problems. As part of the geosciences, neural networks have been used in many applications, including meteorology (Hsieh and Tang 1998; Liu and Weisberg 2011; Liu et al. 2001); oceanography (Dauji et al. 2015; Van der Merwe et al. 2007; Jiang et al. 2018; Krasnopolsky et al. 2016; Deo and Naidu 1998); and hydrology (Lee and Kang 2016, Aichouri et al.; Dawson and Wilby 2001; Sudheer et al. 2002); geophysics (Djarfour et al. 2014; Baddari et al. 2009); space weather (Vandegriff et al. 2005; Vassiliadis 2000; Murray 2018); and environmental science (Haupt et al. 2008; Hsieh 2009; Krasnopolsky 2007, 2013). Due to the large number of parameters to be identified, neural networks present a challenge in addition to their excellent performance. In supervised ANN, the following parameters must be found: the number of hidden layers, the number of neurons in each layer, the type of activation function, the learning rate (b), and the momentum rate (a). As part of the training process, it is crucial to have a sufficient number of neurons in the hidden layer. It may not be possible for a neural network to learn patterns in data if it has only a small number of neurons (underfitting). In contrast, a larger number of neurons in the hidden layer increases the search space dimension, resulting in an increase in generalization failures (overfitting)[2].

2.4.1 Strengths and limitations of geospatial and geophysical data handling

Neural network models have emerged as powerful tools for processing geospatial and geophysical data. These models have several strengths such as their ability to capture complex non-linear relationships within geospatial and geophysical data, to automatically learn relevant features from raw data, to adapt to changes in data distribution over time, and to process large volumes of geospatial data through parallel processing efficiently. As such, they are particularly suitable for tasks requiring high computational power, such as remote sensing image analysis and geophysical signal processing[20].

Nevertheless, neural network models have limitations in handling geospatial and geophysical data. One such limitation is that neural networks require large amounts of labeled training data to learn complex patterns effectively. The limited data availability and high data collection costs in the geosciences can pose significant challenges in this regard. Moreover, despite their high predictive accuracy, neural networks often operate as "black box" models, making it difficult to interpret the underlying relationships between input variables and output predictions. This limitation is critical in geosciences as understanding geological processes and making informed decisions relies on the ability to interpret the underlying relationships[20].

Another limitation is that neural networks are prone to overfitting, particularly when trained on noisy or small datasets. This leads to poor generalization performance on unseen data. Researchers and practitioners need to employ regularization techniques and cautious model selection to mitigate this issue. Finally, training complex neural network architectures, especially deep neural networks with multiple layers, requires significant computational resources and time, posing challenges for real-time applications and large-scale geospatial analysis tasks[20].

In summary, while neural network models offer powerful tools for handling geospatial and geophysical data, researchers and practitioners must consider their strengths and limitations carefully. Appropriate strategies must be employed to address challenges in data availability, model interpretability, overfitting, and computational complexity. The use of neural network models in geosciences requires a deep understanding of their capabilities and limitations to aid in exploring and discovering geospatial patterns and phenomena[20].

2.5 Application of Neural Networks to Well-log Datasets

Luisa Rolon and Shahab D. Mohaghegh(2009) have developed a methodology for generating synthetic wireline logs. This approach analyzes reservoir properties in areas without or incomplete conventional logs. The method uses artificial neural networks (ANNs) together with data from conventional wireline logs. The goal is to reduce companies' costs [24]. The neural network model is developed using a Generalized Regression Neural Network. It incorporates wireline logs from four wells, including gamma ray, density, neutron, and resistivity data. Synthetic logs are generated through two exercises. The first exercise uses all four wells for training, calibration, and verification; the second uses three wells for training and calibration, and the fourth for

verification[24].

Three combinations of inputs/outputs are tested to demonstrate the methodology's robustness. Results show that the combination "A" of inputs/outputs performs the best, followed by "C" and then "B." Data interpolation enhances the accuracy of synthetic logs, indicating the superiority of neural network-based synthesis over conventional approaches such as multiple regression[24].

2.5.1 Well-Logging

Well-logging has been used for almost a century as a vital tool to determine the potential production of hydrocarbon reservoirs. Log analysts interpret the data from the logs to determine the petrophysical parameters of the well. However, for economic reasons, companies do not always have all the logs required to analyze reservoir characteristics [24].

To solve this problem, an approach involving the use of an artificial neural network (ANN) has been developed. The ANN is used together with data obtained from conventional wireline logs to generate synthetic wireline logs for locations where the necessary logs are absent or incomplete[24].

Artificial neural networks have been widely used in reservoir characterization due to their ability to extract nonlinear relationships between sparse sets of data. Studies in this field have used wireline logs and seismic attributes to predict reservoir properties such as effective porosity, fluid saturation, and rock permeability. They also helped to define lithofacies and predict log responses, such as generating synthetic logs. In all cases, it was demonstrated that ANN is a powerful tool for recognition patterns, system identification, and prediction of any variable in the future with a better correlation coefficient (R2) over traditional statistical analysis like linear regression[24].

Mohaghegh et al. (1998) developed a methodology to generate synthetic Magnetic Resonance Imaging (MRI) logs using conventional well logs, such as Spontaneous Potential, Gamma Ray, Caliper, and Resistivity. They used an ANN as their main tool. The synthetic MRI logs were generated with high accuracy, even when the model used data not employed during model development[24].

Mohaghegh et al. (1999) presented an approach that involves neural network design software for low-cost/high-effectiveness log analysis on a field scale. The cost reduction is achieved by analyzing only a group of wells in the field. The intelligent software tool is built to learn and reproduce the engineer's analyzing capabilities on the remaining wells. As part of this study, logs that were missed in several wells and that were necessary for analysis were generated[24].

Bhuiyan (2001) developed a neural network to generate synthetic MRI logs to provide information about the reservoir characteristics of the Cotton Valley formation. Data preparation before network training involved fuzzy logic for grouping well logs together based on similarity criteria of the reservoir formation. This helped to identify the most influential logs for a well. Tonn (2002) used seismic attributes, density, and sonic logs to train an ANN to predict the gamma-ray response of the Athabasca oil sands in western Canada. This helped to solve the reservoir properties and choose the best location to place injection and production wells for a steam injection program[24].

This technique is not intended to eliminate well-logging in a field; it is meant to become a tool for reducing companies' costs when logging proves insufficient and/or difficult to obtain. In addition, this technique can provide a guide for quality control during the logging process by predicting the log's response before the log is acquired [24].

2.5.2 CASE STUDY OF WELL LOGGING

Cao, Fu, and Xu (2022) propose a solution for predicting missing well logs using a neural network model that integrates CNN, BGRU, and self-attention. The model consists of two modules, one that extracts local morphological features and another that captures variation trends. The self-attention mechanism enhances accuracy by assigning weights to highlight relevant information. The approach is effective and practical for real field data from different areas[32]. A model called SAIDNN was developed to predict missing well logs by combining CNNs and BGRU networks. This model extracts local morphological features from the logging data to minimize the loss of historical information and enhance the impact of important data.

According to their results, SAIDNN is the best model for predicting missing well logs, especially at the peak. Considering the local characteristics of well logs and the variation characteristics of the formation, SAIDNN is particularly suited to this task.

For more reliable conclusions, comparing and discussing large datasets from different geological backgrounds is important[32].

A study conducted by Shehata et al.(2021) emphasizes the importance of using artificial neural networks (ANNs) to process and interpret complex geological data. Researchers can holistically analyze various data types using neural networks, such as conventional well logs, core samples, and borehole images. As a result, lithofacies and petrophysical properties of reservoir formations can be more thoroughly characterized.

Researchers can integrate data sets from different scales to capture various geological characteristics and phenomena, such as microscopic properties observed in core samples and macrostructural features observed in borehole images. Using these different sources of information, it is possible to learn and extract patterns from neural networks that may not be apparent when analyzing each type of information separately.

In this integrated approach, one of the key components is the ability to predict lithofacies and petrophysical properties in areas with limited data. To develop predictive models, researchers must train and test neural network models on existing data sets to generalize them to uncored or unexplored regions of the reservoir. Consequently, reservoir heterogeneity can be better understood, and the characterization and modeling of reservoirs can be more accurate.

Accordingly, the study by Shehata, Osman, and Nabawy highlights the potential benefits of neural networks in petrophysical and lithofacies analyses. By integrating multi-scale data sets and using advanced machine learning techniques, researchers can gain a deeper understanding of reservoir properties and behavior, ultimately assisting petroleum industry professionals in making more informed decisions[26].

Tabasi et al. (2022). developed optimized machine-learning models to predict fracture density using conventional good logs in carbonate formations. The hybrid models

significantly enhance fracture density prediction accuracy, including distance-weighted K-nearest neighbor and neural network with firefly and artificial bee colony optimizers. The study's generalizability is confirmed with datasets from two additional wells in the Marun field. Overall, the developed ML algorithms offer a promising solution for predicting fracture density using conventional well logs, providing valuable reservoir characterization and optimization insights. Tabasi et al. developed optimized machine-learning models to predict fracture density using conventional well logs in carbonate formations. The hybrid models significantly enhance fracture density prediction accuracy, including distance-weighted K-nearest neighbor and neural network with firefly and artificial bee colony optimizers. The study's generalizability is confirmed with datasets from two additional wells in the Marun field. Overall, the developed ML algorithms offer a promising solution for predicting fracture density using conventional well logs, providing valuable reservoir characterization and optimization insights. Accurately identifying and characterizing natural fractures are essential for understanding fluid flow dynamics in oil and gas reservoirs, especially in carbonate formations. While information from cores and formation imaging logs is valuable, its availability and cost constraints necessitate alternative methods for predicting fracture density[29].

Using machine learning algorithms, Kheirollahi, Shad Manaman, and Leisi(2023) conducted a study to estimate shear wave velocity in carbonate oil reservoirs. Existing methods are expensive, so the authors aimed to use conventional well logs to develop more cost-effective techniques. They pre-processed various logs, partitioned the dataset, and constructed different models. The feed-forward neural network showed the best results with high R-values of 0.99 and 0.96 for the training and testing datasets. The authors fine-tuned the neural network architecture for enhanced prediction in other wells. This study offers promising avenues for improved reservoir characterization and decision-making in oil and gas exploration and production activities[21].

Sun and his team(2019) have conducted a study on optimizing models for quick and accurate lithology identification while drilling using machine learning. Identifying lithology from well-log data is critical in the petroleum industry, but conventional methods often fail to meet the demands of real-time and accurate prediction, particularly with logging while drilling (LWD) equipment, due to the complex sedimentary environment and reservoir heterogeneity.

The study involved comparing and analyzing three prevalent machine learning algorithms - one-versus-rest support vector machines (OVR SVMs), one-versus-one support vector machines (OVO SVMs), and random forest (RF) - using data from conventional wireline logging (CWL) and LWD in the Yan'an Gas Field. The primary objective of the study was to optimize a practical method for LWD systems.

To simplify the input data dimensions, the researchers conducted correlation analysis on the logging data to derive characteristic parameters for training data. They determined the optimal parameter values for each algorithm through the grid search method and 10-fold cross-validation. They then used the three classifiers to predict lithology on actual LWD data.

The results revealed that the characteristic parameters derived from correlation analysis include AC, CAL, GR, K, RD, and SP logs. The overall classification and

recognition performance of the RF classifier was found to be superior to the other two classifiers, with an accuracy exceeding 90%. Although both OVR SVMs and RF classifiers exhibited lower prediction errors than the OVO SVMs classifier for individual lithology identification, the RF classifier notably expedites the training process.

Through comprehensive analysis, the RF classifier was identified as the optimal choice for lithology identification while drilling, offering a blend of short training time and high recognition accuracy. These findings not only advance drilling steering in oilfield development but also contribute valuable insights for future research endeavors in the field[28].

2.5.3 Challenges and Opportunities in Well-Log Interpretation

In petroleum exploration and development, neural networks can be used to interpret well-log data.

Challenges:

A region's geology can be highly complex, with small variations in lithology and porosity. To capture these complexities, neural networks must be trained on several geological scenarios. Well-log data quality and quantity vary dramatically between wells and regions. Data augmentation and preprocessing can improve neural network performance with insufficient or noisy data. Many neural networks are considered 'black boxes, meaning their internal workings are not easily understandable. This lack of transparency can limit the model's usefulness in decision-making, as it makes it difficult to understand how it makes predictions. Neural networks tend to overfit, particularly when dealing with complex geological formations. Model selection and regularization techniques are crucial to minimizing this risk[15].

Opportunities:

Neural networks can learn complex patterns and relationships within data. By identifying subtle correlations between different well-log measurements, more accurate lithology predictions can be made. Automating interpretation with neural networks reduces the need for manual intervention and speeds up analysis workflows. A large-scale exploration and development project can greatly benefit from this. In addition to seismic data and core analysis, neural networks can be integrated with other sources of geological data to achieve a more accurate interpretation. Neural networks can continuously learn new data. As more well-log data becomes available, neural networks can adapt to changing geological conditions and improve performance[15].

As a result, neural networks can potentially improve well-log accuracy, efficiency, and automation, making them a valuable tool for the petroleum industry. With careful consideration of data quality, model complexity, and interpretability, neural networks can provide valuable insight into subsurface geology. In the field of petroleum exploration and development, neural networks present both challenges and opportunities[15].

2.6 Review of ground thermal properties and neural networks

According to Soteris A. Kalogirou (2000), an artificial neural network (ANN) can solve complex and undefined problems across a wide range of domains. An ANN

learns from examples, handles noisy and incomplete data, solves nonlinear problems, and makes predictions quickly. ANNs are used in robotics, pattern recognition, forecasting, medicine, power systems, manufacturing, optimization, signal processing, and social sciences. In system modeling, ANNs facilitate complex mapping and system identification.

It emphasizes thematic relevance over chronological order in exploring neural network applications in energy-related issues. Kalogirou uses ANNs to model and design solar steam-generating plants, estimate parabolic-trough collector parameters, and predict solar water-heating systems' performance. ANNs can also be used to predict airflow in naturally ventilated rooms and energy consumption for passive solar buildings with multiple hidden layers. In other fields of energy production and consumption, ANNs are suitable for modeling.

Fellow researchers in the energy domain have applied ANNs to heating, ventilation, and air conditioning systems, solar radiation analysis, power generation systems, load forecasting, and refrigeration[19].

Adelina P. Davis and Efstathios E. Michaelides(2009) have conducted a rigorous simulation to assess the feasibility of exploiting abandoned oil wells as a source of geothermal power. The proposed method entails injecting and retrieving a secondary fluid, namely isobutane, into the well at moderate pressures to produce vapor. The simulation employs a computational model that incorporates mass, energy, and momentum conservation equations for well flow, allowing the team to determine the fluid's state from injection to retrieval.

The study's results indicate that these systems can achieve a maximum power output that is dependent on the temperature at the well bottom and injection pressure. In the South Texas region, where typical wells have been examined, there is potential for generating electric power between 2-3 MW. The research findings, therefore, offer promising prospects for the utilization of geothermal energy and the recovery of otherwise abandoned oil wells[8].

Abandoned oil wells have the potential to generate power when modified into double-pipe heat exchangers. Injecting a secondary fluid like isobutane at the outer rim can increase the power output. A single well can produce over 3MW of power with a 450 K bottom-hole temperature and 30 bar injection pressure. This energy source is not intermittent and can be available for both peak and basic demands. The power output depends on down-hole temperature, injection pressure and velocity, and pipe geometry. Optimal injection pressure is 30 bar, and a one-inch insulation thickness helps maintain fluid temperature. When injection velocity and inner radius of the pipe are optimized, power output can reach 3.4MW[8].

In the study conducted by A. Hartmann, V. Rath, and C. Clauser,(2005) the authors focused on investigating the correlation between thermal conductivity and other petrophysical properties in a borehole drilled within a Tertiary Flysch sequence. The authors were able to establish a set of equations that predicts rock thermal conductivity using logging data, with an average accuracy of better than 0.2 W/(mK), through regression analysis of thermal conductivity, bulk density, and sonic velocity.

The authors then utilized logging data to calculate a lithological depth profile and

subsequently employed it to develop a thermal conductivity profile. By comparing the conductivity-depth profile with laboratory data, the authors determined that thermal conductivity can be computed with an accuracy of less than 0.3 W/(mK) using conventional wireline data. Furthermore, the author's comparison of two different models demonstrated the practicality of this approach, even when using old and incomplete logging data.

In conclusion, the study provides valuable insights into the prediction of thermal conductivity for boreholes that lack appropriate core data in similar geological settings. The authors' findings are of great importance to the field and demonstrate the potential for further research to refine this approach[16].

In their scholarly article, Fred F. Farshad, James D. Garber, and Juliet N. Lorde(2000) present a novel approach that employs artificial neural networks (ANNs) to predict temperature profiles in oil wells, with a specific focus on 27 wells situated in the Gulf of Mexico. The authors develop two ANNs capable of forecasting the temperature of the fluid flowing at any depth within these wells by utilizing back propagation for network training. Through testing with measured temperature profiles from the 27 oil wells, both neural network models demonstrate the ability to effectively capture the general temperature profile trends observed in naturally flowing oil wells, achieving an impressive accuracy with a mean absolute relative percentage error of 6.0%.

The authors compare the accuracy of their proposed neural network models with existing correlations that are used to predict temperature profiles in well-bore fluids. The various correlations developed based on theoretical principles such as energy, mass, and momentum balances coupled with regression analysis. The Neural Network 2 model notably demonstrates significantly lower mean absolute relative percentage error than other correlations. Furthermore, the accuracy of the neural network models is compared to Kirkpatrick's correlation to provide further validation of their efficacy[11].

Rahman Ashena(2023) proposes an innovative idea of converting inactive or abandoned oil and gas wells into geothermal wells. This would harness geothermal energy and defer the costs associated with their closure. To validate the feasibility of this proposal, Ashena conducted a detailed analysis of 20 case studies from different countries.

The analysis focuses on various key aspects, such as formation characteristics, downhole parameters, and surface conditions. Further, it delves into different production scenarios, such as open-loop and closed-loop systems, optimization techniques for open-loop systems, borehole heat exchangers, insulation methods, and the benefits of installing bottom hole curvature.

The study also covers the use of organic Rankine cycle (ORCs), selection of circulation fluids, circulation rates, working fluids, and performance metrics such as coefficient of performance (COP) and thermal efficiency.

Ashena concludes by recommending a tailored idea for super-highly pressured aquifers, emphasizing the vast potential of utilizing geothermal energy from abandoned and old petroleum wells. This comprehensive investigation sheds light on the feasibility and efficiency of repurposing oil and gas wells for geothermal energy production[3].

A. Bassam and colleagues(2010) employ an artificial neural network (ANN) approach to develop a predictive model for estimating static formation temperatures

(SFT) in geothermal wells. They successfully train a three-layer ANN architecture using a database of geothermal borehole data, which includes statistically normalized SFT estimates derived from seven commonly used analytical methods in the geothermal industry.

The main input variables for training the ANN include bottom-hole temperature (BHT) measurements and shut-in times, while transient temperature gradients serve as secondary variables. The LevenbergMarquardt (LM) learning algorithm, hyperbolic tangent sigmoid transfer function, and linear transfer function are utilized to optimize the ANN.

The best training dataset yields an ANN architecture composed of five neurons in the hidden layer, achieving a satisfactory prediction efficiency with a correlation coefficient (Rš) of 0.95. The ANN model demonstrates a percentage error of less than 75%, indicating suitable accuracy. The predicted SFTs from the ANN model are statistically analyzed and compared with true SFT data obtained from synthetic experiments and actual BHT logs collected in geothermal boreholes during long shut-in times.

The results indicate strong agreement (Rš = 0.95) between the SFT estimates inferred from the ANN model validation process and the true SFT data reported for synthetic and field experiments. This suggests that the new ANN model could serve as a practical tool for reliably predicting SFT in geothermal wells using only BHT and shut-in time as input data[4].

A. Bassam and colleagues(2013) employ an artificial neural network (ANN) approach to develop a predictive model for estimating static formation temperatures (SFT) in geothermal wells. They successfully train a three-layer ANN architecture using a database of geothermal borehole data, which includes statistically normalized SFT estimates derived from seven commonly used analytical methods in the geothermal industry.

The main input variables for training the ANN include bottom-hole temperature (BHT) measurements and shut-in times, while transient temperature gradients serve as secondary variables. The LevenbergMarquardt (LM) learning algorithm, hyperbolic tangent sigmoid transfer function, and linear transfer function are utilized to optimize the ANN.

The best training dataset yields an ANN architecture composed of five neurons in the hidden layer, achieving a satisfactory prediction efficiency with a correlation coefficient (Rš) of 0.95. The ANN model demonstrates a percentage error of less than 75%, indicating suitable accuracy. The predicted SFTs from the ANN model are statistically analyzed and compared with true SFT data obtained from synthetic experiments and actual BHT logs collected in geothermal boreholes during long shut-in times.

The results indicate strong agreement (Rš = 0.95) between the SFT estimates inferred from the ANN model validation process and the true SFT data reported for synthetic and field experiments. This suggests that the new ANN model could serve as a practical tool for reliably predicting SFT in geothermal wells using only BHT and shut-in time as input data.

Sven Fuchs and Andrea Förster have conducted research to explore methods for predicting rock thermal conductivity (TC) using well-log data, with a focus on the North

German Basin. TC data is an essential factor in understanding subsurface temperature dynamics and heat flow. However, obtaining drill cores for laboratory measurements can be challenging. Hence, the researchers investigated the correlation between TC and standard well-log data, including gamma ray, density, sonic interval transit time, hydrogen index, and photoelectric factor.

The study used both theoretical analysis and real subsurface data from four boreholes to examine the correlation trends between TC and well-log responses for different mineral assemblages and porosity levels. The researchers proposed empirical equations for predicting matrix TC separately for different sedimentary rock groups. The input parameters for the equations include the volume fraction of shale, matrix hydrogen index, and matrix density. The error of matrix TC prediction ranges from 4.2% to 11.4% for different rock types.

Furthermore, the researchers developed prediction equations for bulk TC based on lithological compositions. The input parameters for these equations include the volume fraction of shale, hydrogen index, and sonic interval transit time. These equations predicted TC with average errors ranging from 5.5% to 11% for various lithologies. The validation using measured temperature logs and modeled temperature logs demonstrated excellent agreement, with interval temperature gradients varying by less than 3 K km1 and predicted absolute temperatures fitting with less than 5% accuracy.

Compared to previous TC prediction approaches, the developed equations showed significantly higher prediction accuracy, with average errors less than 10%. This study provides valuable insights into predicting TC from well logs in sedimentary formations, offering improved accuracy for subsurface temperature estimation[12].

The team of Goutorbe, Lucazeau, and Bonneville(2006) introduces a novel technique for estimating the thermal conductivity of sedimentary rocks. This technique utilizes neural networks trained on geophysical well logs. Their approach, calibrated on Ocean Drilling Program (ODP) data, involves the use of thousands of conductivity measurements and five key geophysical well logs, including sonic, density, neutron porosity, resistivity, and gamma-ray.

The researchers have employed multilayer perceptrons (MLP) to establish an empirical relationship between these well logs (MLP inputs) and thermal conductivity (MLP output). Validation tests have demonstrated that MLPs provide more accurate conductivity estimates compared to traditional linear models, achieving results within a 15% confidence level. Notably, even when utilizing only four well logs, including neutron porosity, MLPs still yield satisfactory results.

The authors have compared MLP predictions with conventional 'mixing' methods in two ODP sites. While the mixing technique produces reliable outcomes with precise rock descriptions, MLPs offer a more straightforward alternative, requiring no additional parameters and delivering predictions in strong agreement with experimental trends.

The proposed method holds great promise for estimating heat flow from data collected in both scientific and industrial boreholes. By harnessing the power of neural networks, Goutorbe, Lucazeau, and Bonneville have offered a valuable tool for enhancing thermal conductivity estimation in subsurface exploration and geothermal energy

applications[14].

A team of researchers led by Dalla Santa(2020) has created a comprehensive database of thermal properties crucial for the design of ground source heat exchanger (GSHP) systems. This Decision Support System is part of the EU-funded Cheap-GSHPs project and provides essential underground thermal property input data for sizing geo-exchange systems.

The database integrates information from various sources, including international guidelines, extensive literature reviews, and over 400 direct measurements. Although the database primarily focuses on thermal conductivity data, it does not include the convective contribution facilitated by groundwater flow to heat transfer. In their paper, the authors present and analyze the compiled database, shedding light on its significance for GSHP applications.

The DSS developed within the scope of the European project Cheap-GSHPs is an efficient tool for stakeholders involved in the planning and design of closed-loop Ground Source Heat Pump (GSHP) systems. This system integrates crucial aspects that are significant for designing such systems, thereby providing users with necessary design parameters through software tools linked to a series of datasets.

Thermo-geological properties, particularly the local thermal properties of the ground and the ground temperature profile play a pivotal role in the design of ground heat exchangers. These properties determine thermal exchange capacity, impact the overall performance of the energy system, and influence investment. The UNIPD Cheap-GSHPs database for geological materials serves as an international reference for thermal properties in shallow geothermal systems. It integrates practical purposes by offering necessary thermal property values of geological conditions through a dedicated database developed as part of the Cheap-GSHPs project. This data is invaluable for preliminary GSHP feasibility studies and design processes. Key elements of this database include:

The UNIPD Cheap-GSHPs database for geological materials serves as an international reference for thermal properties in shallow geothermal systems. It integrates widely used data from sources such as VDI and ASHRAE guidelines, along with additional literature references. Over 250 samples of unconsolidated sediments and rock were measured to enhance existing literature datasets. The database recommends values calculated as averages from literature and project measurements, alongside minimum and maximum values, to illustrate thermal conductivity variations due to natural material heterogeneity. The introduction of new data expands the literature's variability range for the thermal conductivity of phyllite while more precisely defining ranges for andesite, trachyte, and serpentinite. A new dataset for volume-related specific heat capacity is included for specific lithotypes. Thermal properties for unconsolidated sediments are categorized based on granulometry and moisture content for practical application. Updated data on the thermal properties of gravels, obtained using an improved device developed as part of the project, are included in the database, providing a significant addition to internationally published data. It is important to note that these values represent thermal conductivity and do not account for convective contributions from groundwater flow[7].

Maher Nasr, Jasmin Raymond, Michel Malo, and Erwan Gloaguen conducted a

study using well log analysis to assess the geothermal potential of the St. Lawrence Lowlands sedimentary basin. The study aimed to address the challenge of determining thermal conductivity, heat flow, and temperature in sedimentary basins due to the heterogeneous distribution of minerals across various rock types. This is particularly difficult when relying exclusively on databases from the oil sector.

To overcome this challenge, the study developed a novel methodology that utilizes well-log data to improve the inference of thermal conductivity variations in sedimentary formations. This approach enables the evaluation of heat flow and temperature extrapolation at depth. The methodology was specifically applied to the St. Lawrence Lowlands basin, leveraging available oil and gas databases, although it was not originally intended for geothermal exploration.

The methodology involved a quantitative analysis of well log data with an inversion approach based on limited reference wells. Empirical relationships were established to calculate thermal conductivity profiles for each available well. Pressure and temperature corrections were applied, and continuous logs of thermal conductivity were utilized to estimate Earth's heat flux density using bottomhole temperatures and to extrapolate temperatures at depth.

To achieve this, the study solved a modified version of Poissons equation using the finite difference method. The results indicated an average temperature and standard deviation for the St. Lawrence Lowlands at depths of 1000m, 2500m, and 5000m, approximately 32 ś 6.9 řC, 63 řC ś 12.7 řC, and 119 řC ś 28.3 řC, respectively. Additionally, temperature ranges were observed to vary from 19 to 52 řC, 41 to 112 řC, and 75 to 236 řC at depths of 1000m, 2500m, and 5000m, respectively[22].

2.6.1 Review of the literature related to geothermal energy advancements

An overview of various studies exploring geothermal energy utilization and thermal properties assessment is presented through a literature review.

Artificial neural networks (ANNs) have been identified as a promising solution to complex problems related to energy utilization. Researchers, such as Soteris A. Kalogirou, have highlighted the versatility of ANNs in different applications, including predicting thermal profiles in oil wells and estimating static formation temperatures (SFT) in geothermal wells.

Studies by Adelina P. Davis, Efstathios E. Michaelides, and Rahman Ashena have explored the feasibility of converting abandoned oil wells into geothermal power sources. Techniques involving injecting secondary fluids, such as isobutane, into wells can generate significant power output, contributing to the utilization of geothermal energy and repurposing inactive oil wells.

Prediction of thermal conductivity has been a key research area for understanding subsurface temperature dynamics. Studies by A. Hartmann, V. Rath, and C. Clauser, as well as Sven Fuchs and Andrea Förster, have demonstrated methodologies using well-log data and neural networks to predict thermal conductivity with high accuracy, aiding in subsurface exploration and geothermal energy applications.

Comprehensive databases, such as the one developed by Giorgia Dalla Santa and colleagues, provide essential thermal property values for designing ground source heat

exchanger systems. The integration of data from various sources, including international guidelines and direct measurements, aids in preliminary feasibility studies and design processes for GSHP systems.

Studies like Maher Nasr et al. have assessed the geothermal potential of sedimentary basins using well-log analysis. Researchers have developed novel methodologies to overcome challenges in determining thermal conductivity and temperature profiles, providing insights into the feasibility of utilizing geothermal energy from such basins.

In conclusion, the literature review underscores the importance of innovative approaches, data integration, and advanced technologies in harnessing geothermal energy and understanding subsurface thermal properties for sustainable energy applications.

The exploration and utilization of geothermal energy is a vital field, and studying ground thermal properties is essential for its advancement. However, obtaining accurate thermal property data can be challenging, especially in areas where direct measurements are limited or unavailable. To address this issue, leveraging well-log datasets and advanced computational techniques like neural networks can provide valuable insights into ground thermal properties, aiding in the development of sustainable geothermal energy solutions. Therefore, the objectives of this study are to evaluate the feasibility of using neural networks to analyze well-log datasets for predicting ground thermal properties, develop and optimize neural network models that accurately estimate thermal conductivity, heat flow, and temperature profiles based on well-log data, investigate the potential of neural network-based approaches to improve the resolution and accuracy of ground thermal property predictions compared to traditional methods, validate the performance of the developed neural network models using real-world well-log data from diverse geological settings, and explore the implications of the study findings for the design, implementation, and optimization of geothermal energy systems, with a focus on enhancing efficiency and sustainability[19].

2.7 Understanding the importance of oil and gas well data for predicting thermal conductivity.

2.7.1 Oil window

The temperature required for the production of oil and gas depends on various factors, such as the depth and composition of the reservoir and the type of hydrocarbons present. Generally, oil and gas formation occurs over millions of years under specific geological conditions characterized by high temperatures and pressures.

Petroleum formation typically occurs several kilometers below the Earth's surface at temperatures ranging from 60 to 120 degrees Celsius (140 to 248 degrees Fahrenheit). Here, organic matter, such as plankton and algae, undergoes burial and transformation into hydrocarbons due to heat and pressure.

Similarly, natural gas formation can occur at similar depths but may necessitate slightly higher temperatures, ranging from about 90 to 150 degrees Celsius (194 to 302 degrees Fahrenheit). While natural gas is mainly composed of methane (CH4), it can also contain ethane, propane, and other hydrocarbons.

In some cases, higher temperatures and pressures found at greater depths or in geologically active areas can lead to the creation of thermogenic gas and oil, which have undergone more extensive thermal maturation processes.

It's essential to note that these temperature ranges are approximate and are subject to geological factors, such as the presence of organic-rich source rocks, the thermal conductivity of surrounding formations, and the duration of heating. Understanding the temperature conditions within a reservoir is critical for assessing its potential for oil and gas production and optimizing recovery techniques[31].

2.7.2 Importance of thermal conductivity

Understanding the thermal conductivity of formations within a reservoir is of utmost importance for several reasons. Firstly, thermal conductivity plays a crucial role in heat transfer through the reservoir rocks, determining how efficiently heat can propagate. As temperature significantly influences the generation, maturation, and migration of hydrocarbons, higher thermal conductivity can help inform the thermal history of the reservoir and hydrocarbon generation processes.

Secondly, knowledge of thermal conductivity is valuable for reservoir characterization and understanding the thermal properties of the rocks. This information is especially useful for predicting temperature distributions, hydrocarbon generation rates, and reservoir behavior over time, which helps with reservoir modeling and simulation studies.

Thirdly, thermal conductivity impacts the temperature distribution within the reservoir during production operations. Thus, understanding these temperature profiles can help optimize hydrocarbon recovery by informing decisions regarding production strategies, such as well placement, injection rates, and fluid properties.

Fourthly, reservoirs with high thermal conductivity may also have the potential for geothermal energy extraction. Understanding subsurface thermal properties is vital for assessing the feasibility and efficiency of geothermal projects[6].

3

Methodology

3.1 Data Sources

Three distinct oil fields in Iran were used to collect well-log data: The first formation is located in the southwest of Iran, the second Field is in the west of Iran, and the third Field is in the south of Iran. Ten wells were made from these data.

3.2 Dataset Description

First oil field

- Location: Southwest Iran.Figure3.1
- Lithology: Heterogeneous, including Anhydrite, Dolomite, Limestone, Sandstone, and Shale.
- Depth Range: 3400 to 3800 meters.
- Temperature: The bottom log interval temperature is 115 °C, and the top log interval temperature is 98 °C.
- Drilling Bit Size: 8.5 inches.
- The density of Drilling Fluid: 9 lb/gal.
- Frames: Each log consists of 1771 frames.

Second oil field

- Location: West Iran.Figure3.2
- Lithology: Interpretation results show that the Sarvak Formation has hydrocarbon potential, and the average useful porosity in studied reservoir intervals is about 12%. Due to the formation's high-energy environment, the shale volume is low.
- Depth Range: 3187 to 4280 meters.
- Temperature: Bottom hole temperature is 138°C.
- Frames: Each log consists of 7107 frames.

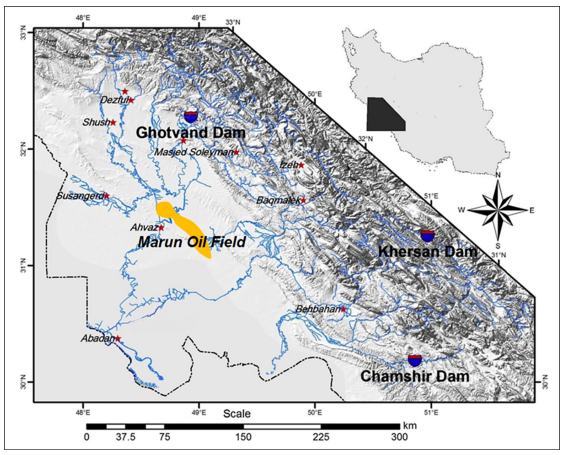

Figure 3.1: The location of the first oil field in southwest Iran[23]

3.2.1 Third oil field

- location: south of Iran.Figure3.3
- Lithology:
  - 0-10% Limestone,
  - 10%-50% Dolomite limestone,
  - 50%-90% Calcareous dolomite,
  - 90%-100% Dolomite
- Texture: Peloidal grainstones are well structured and winnowed. Intraclastic grainstones are poorly sorted and bimodal.
- Sedimentary Structures: Planar bedded grainstones with local soft-sediment folds; planar bedded mudstones/wackestones.
- Biogenic: Dominated by Zoophycos burrows, with algal binding and other burrow forms.
- Depositional Environment: Lagoon to tidal flat setting with grainy washovers and local tidal inlets, transitioning upwards into a sabkha/salina setting.
- Depth Range: 2800 to 3200 meters.
- Frames: Each log consists of 3123 frames.
- Temperatur Range: 85°C to 105°C

3.2.2 Types of Well-Log Data

The datasets include various types of well-log measurements, such as:

- Gamma-Ray logs
- Caliper logs
- Resistivity logs
- Sonic logs
- Neutron porosity logs
- Density logs
- Total porosity logs
- Photoelectric factor logs

Sample Rate: Data was recorded at a sample rate of 0.15 seconds.

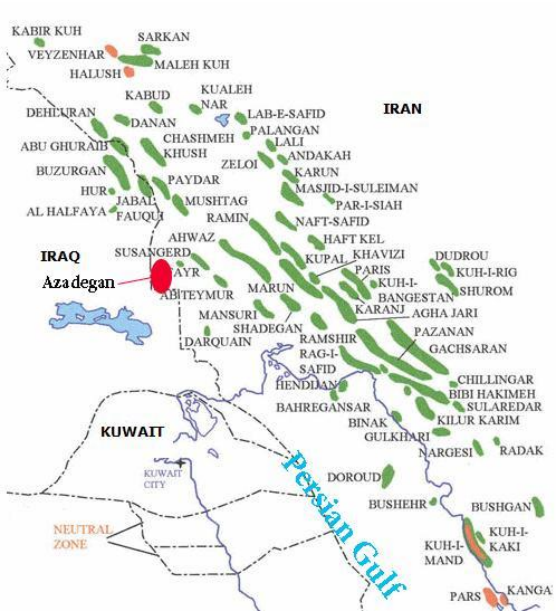

Figure 3.2: Position of the second oil field in Iranian oil filed mapp[25]

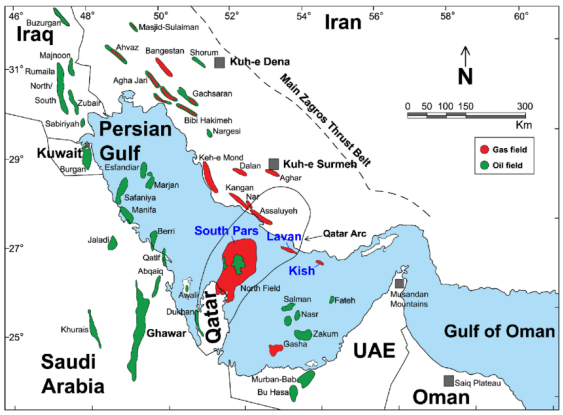

Figure 3.3: Location of third oil field[18]

3.3 Data Preprocessing

3.3.1 Introduction to GeoLog

GeoLog is a comprehensive software suite for processing and interpreting well-log data. It includes tools for quality control, data editing, and advanced modeling. The importance of well-log editing cannot be overstated. Editing well-log data is crucial to ensure accuracy and reliability in subsequent analyses. Raw well-log data often contain noise, errors, and inconsistencies due to tool malfunctions, environmental conditions, or human error. Proper editing helps remove these anomalies and enhance the data quality.

3.3.2 Data Import

Importing well-log data into software platforms like Leapfrog Geothermal involves gathering data from various sources, such as files (CSV, ASCII, LAS), databases, or specialized software (e.g., acQuire, iPoint), and matching the data in the selected files with the expected columns for each type of table (e.g., collar, survey, interval, screens) to ensure proper structuring and recognition by the software; the data must be in the specific formats expected by the software, typically CSV, ASCII, or LAS, and the well ID must be consistent across all tables for the data to be properly associated and linked together, allowing the software to recognize all the data belonging to a specific well; after the import, it's important to visually inspect the data to ensure it has been correctly imported and that there are no obvious issues or discrepancies, laying the foundation for further analysis and interpretation. GeoLog enables the import of well-log data from various formats, such as LAS and DLIS. Users can import data from multiple wells and fields for comprehensive analysis.

3.3.3 Quality Control (QC)

Quality control (QC) of well-log data ensures the reliability and accuracy of the data used in oil and gas exploration and production. Well-log data forms the foundation for evaluating oil and gas reserves and making critical decisions in the industry. Poor-quality data can lead to erroneous conclusions and costly mistakes

3.3.4 Depth Matching

For alignment, use a common depth scale. To interpret logs correctly, all depth intervals must match. In sandstone and shale formations, the gamma-ray log is used as a reference to match other logs. However, the density or neutron log is used as the reference in carbonates. The tools available in the GeoLog software matched petrophysical logs in the studied wells from the Asmari formation, such as depth-matching the sonic log to the density log.

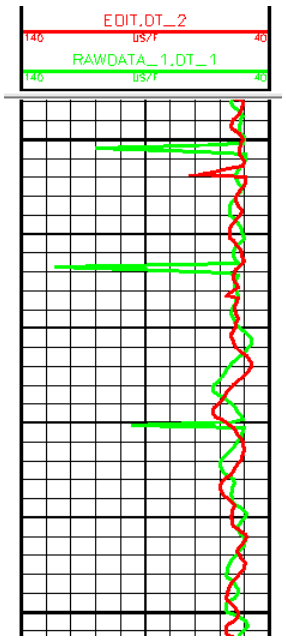

Figure 3.4: Despiking on the sonic log (The red one is corrected)

3.3.5 Noise Reduction and Despiking

In dense, high-velocity formations like anhydrite, which is considered a cap rock, low transit times can cause spikes in the sonic log. These spikes are due to receiver measurement errors and are unrelated to the formation's rock properties. This phenomenon is known as cycle skipping. The Despiking tool in the GeoLog software removes the noise generated in the sonic log (depicted in green), resulting in the corrected sonic log (depicted in red) as shown in Figure3.4

3.3.6 Smoothing

Noises created by tool sticking, cable stretching, or device shutdown at certain depths of the well and zones with fractures can cause density and neutron logs to show step-like spikes. These spikes can affect the calculations of petrophysical parameters. The logs were smoothed in these wells using the Smooth tool in the GeoLog software. Log data may be smoothed to remove anomalous values. The Smooth module has four smoothing methods: mean, median, harmonic, and geometric. The size of the smoothing filter, or number of smooth points, determines the window length. The higher the number of sampling points, the greater the smoothing. Smooth only applies a box filter. The weights of each sample point are uniform. The number of points smoothed about a particular sample point includes the current one and should always be an odd number.

3.3.7 Precalculation

The precalc module is a compulsory precursor to any petrophysical analysis for several reasons:

- Some environmental corrections are dependent on mud cake thickness. Commonly, the mud cake thickness measured on the density/neutron porosity curves

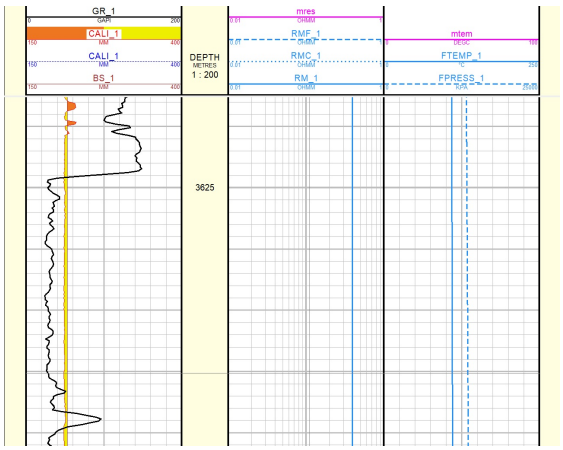

Figure 3.5: precomp layout after running precalc module

and the resistivity curves will be different. The pre-processing option creates mud cake thickness curves for both of these tools.

- The photoelectric absorption cross-section (U) will be calculated as the product of the photoelectric index and electronic density. This will be overwritten if environmental corrections are subsequently applied to the density log.
- Various fluid properties that are used by Multimin are dependent on both the mud pressure in and the temperature of the borehole and the immediately surrounding rock. Some environmental corrections also use these parameters. The precalc module places curves of these calculated properties into the database.
- Conductivities for the flushed zone (CXO) and unflushed zone (CT) will be calculated from the deep and shallow resistivity logs as they are listed in the alias. alias file. These will be overwritten if environmental corrections are subsequently applied to the resistivity logs.
- Mud, mud cake, and mud filtrate resistivities from samples need to be translated into resistivity curves that vary with depth and temperature

The PRECALC module is used to calculate the following parameters from well-log data (Figure3.5):

- Formation temperature and pressure profiles.
- Formation temperature and pressure profiles.
- Formation temperature and pressure profiles.
- Downhole mud properties (Rmf, Rm, Rmc) from sample measurements.
- Salinities of mud and mud filtrate from sample measurements.
- Mudcake thicknesses for both resistivity and porosity tools.
- Photo-electric absorption cross-section: U
- Conductivities of unflushed and flushed zones (Ct, Cxo) from measured resistivities.

These items are determined in Geolog for all wells.

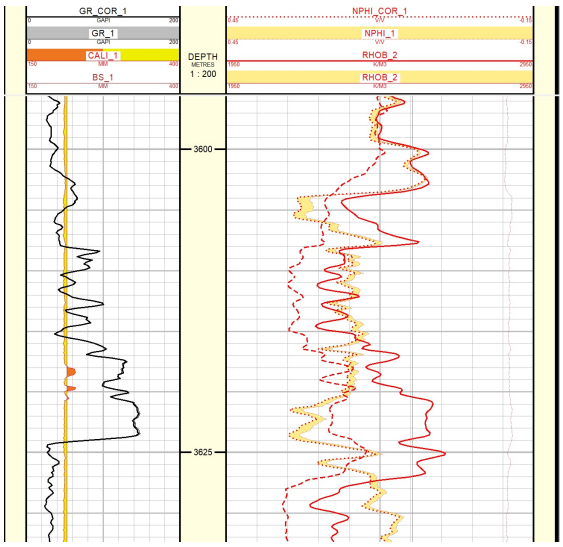

Figure 3.6: Layout of Environmental Corrections

3.3.8 Environmental Corrections in Geolog

Raw data indicates the formation of rock and fluid properties and is strongly influenced by the type of environment the tools are exposed to at the time of data acquisition. Hence, the raw data needs to be corrected, resulting in a set of log data that is consistent across the same formation, regardless of the environment. Some conditions that can affect the tool responses are mud properties (salinity, barites in mud, conductive of mud, etc.), borehole size, and even tool orientation. Various correction charts are available depending on the tool used to record the data. These charts are usually generated and supplied by the service provider. Sometimes, the service provider supplies environmentally corrected data; other times, the end user must apply corrections by selecting the appropriate charts for the tool. Environmental corrections are applied during phase rotation of the real and imaginary data.(Figure3.6)

- **Salinity Correction:** The salinity correction is only applied if the Rmf < 10 ohm.m at 75°C. The correction compensates for the loss of hydrogen atoms replaced by salt ions.
- **Temperature Corrections:** Temperature affects protons' thermal relaxation and reduces the returned signal's amplitude. The temperature correction should always be applied.
- **Hydrogen Depletion Correction:** Increased formation temperature reduces the formation fluid's density and decreases the hydrogen index. Higher pressures increase the hydrogen index. This effect is compensated for by using a Hydrogen Depletion Multiplier, which is a function of porosity and temperature

In this section, the Schlumberger Charts book is used for Environmental Corrections of well-log data, and it applies to GR, neutron, density, and resistivity logs.

3.3.9 Determining of petrophysical parameters

Within Geolog, Determin provides advanced deterministic formation evaluation solutions for petrophysicists, geologists, and engineers. Determin is a comprehensive suite of individual deterministic modules that allow the analyst to apply all the major

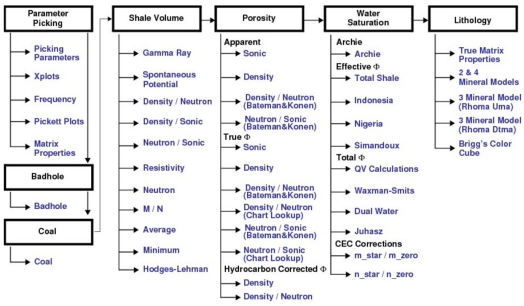

Figure 3.7: Flow chart of determining of petrophysical parameters

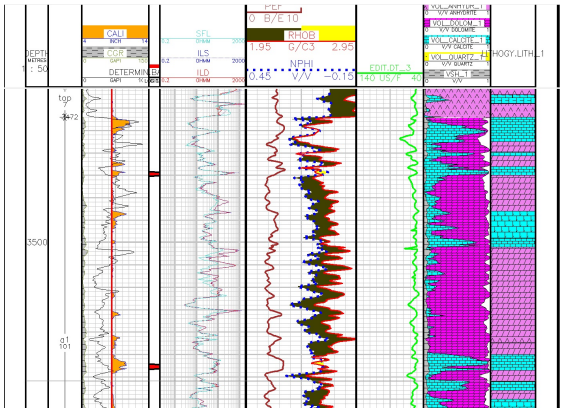

Figure 3.8: layout of Determination Analysis of first oil field

modern petrophysical models in the traditional analysis methodology. It includes all common techniques for determining shale/clay volumes, porosity, saturation, and lithology. Interactive parameter picking and multi-zone/multi-well analysis provide a rapid workflow for formation evaluation. The Petrophysics menu provides a variety of modules for performing deterministic petrophysical analysis. Modules have been constructed to incorporate the concept of total and effective porosities and saturations, illustrated in Figure3.7

3.3.10 LAYOUT OF DETERMINATION ANALYSIS OF FIRST OIL FIELD

As can be seen in the picture, the first track shows CGR, GR, and CALIPER logs. The next track shows resistivities logs, followed by density logs, neutron logs, and photoelectric factor logs, and finally, sonic logs are displayed. These logs determine and correlate the lithology track with the core data's lithology. The formation is heterogeneous, and the lithology includes Anhydrite, Dolomite, limestone, sandstone, and shale(Figure3.8 and 3.9).

3.3.11 LAYOUT OF DETERMINATION ANALYSIS OF SECOND OIL FIELD

In the second field, lithology is limestone without any shale, and we can say pure limestone.(Figure3.10)

3.3.12 LAYOUT OF DETERMINATION ANALYSIS OF THIRD OIL FIELD

In this oil field, we have Dolomite, Limestone, and layers of Anhydrite.(Figure3.11)

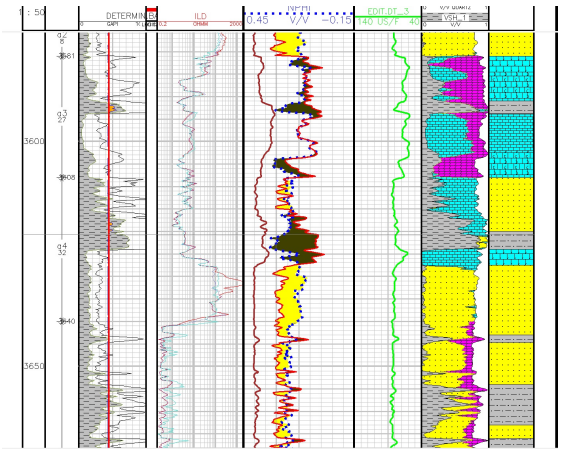

Figure 3.9: layout of Determination Analysis of first oil field

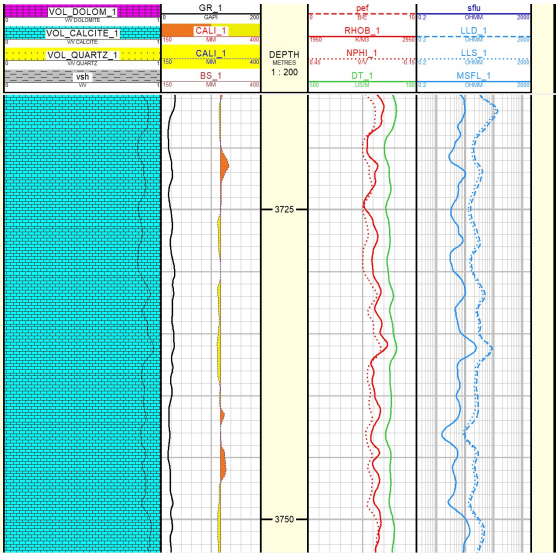

Figure 3.10: layout of Determination Analysis of second oil field

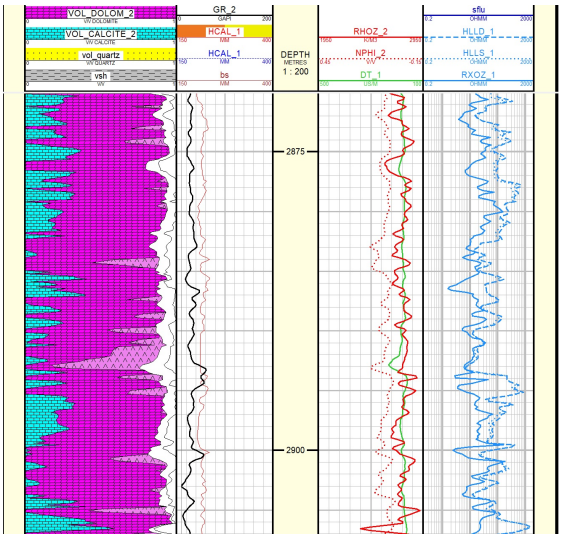

Figure 3.11: layout of Determination Analysis of third oil field

Vol. Dol	Vol. Lim	Vol.sh	Vol.sand	Vol.Ahy
0.34	0.14	0.18	0.34	0.02

Figure 3.12: Volume of Each lithology

3.4 Estiamtion of thermal conductivity

In the Geolog, the porosity and volume of lithology are determined for each well. The volume of lithology in well-1 from the first oil field is shown in figuure3.12

$$\log(\lambda) = \sum_{i=1}^{n} V_i \cdot \log(\lambda_i) \tag{3.1}$$

In this equation:

λ represents the thermal conductivity of the host rock.

V_i represents the volumetric fraction of the component.

λ_i represents the thermal conductivity of the component.

I calculated the thermal conductivity profiles for the formation using the geometric average method, which involves weighting each component's contribution to thermal conductivity by its volumetric fraction. I used the recommendations from the paper "An updated ground thermal properties database for GSHP applications" by Galgaro et al. (2020) to compute the thermal conductivity values.(Figure3.14) With the help of Python(Figure3.13), I processed the well-log data and volumetric fractions to determine the thermal conductivity profiles for the geological formations under consideration.

The next step involves importing this data into Geolog software after predicting thermal conductivity using the formula provided. Thermal conductivity data can be visualized along with other well-log data, such as gamma ray, resistivity, neutron, density, sonic, and photoelectric factor logs, in Geolog. This method can also be used to analyze thermal conductivity in conjunction with other geological parameters.

3.4.1 verifying thermal conductivity calculated with measured values in the Laboratory

I used Anhydrite, limestone, sandstone, organic shale, organic sandstone, and dolomite samples to validate the estimation values. (Figure3.15) I utilized the Isomet 2114 device in the University of Padova laboratory to determine the samples' thermal conductivity.(Figure3.16) The results are presented in Table 2 and can be seen in the following figure3.17

3.4.2 ISOMET 2114

The ISOMET 2114 is a portable hand-held measuring instrument for directly measuring heat transfer properties of a wide range of isotropic materials, including cellular insulating materials, plastics, glasses, and minerals. It has two optional measurement probes: needle probes for soft materials and surface probes for hard materials. It applies a dynamic measurement method, which reduces the measurement time compared to

```python
import pandas as pd
import numpy as np
dLoc = 'D.csv'
df = pd.read_csv(dLoc)
ddf = df.dropna(how="all", axis=1)
ddf.insert(4,'1value',1)
print(ddf)
gLoc = 'G.csv'
gdf = pd.read_csv(gLoc, header= None)
newRow = [1,1,1,1,1]
gdf.loc[len(df)] = newRow
gdf = gdf._append(newRow, ignore_index=True)
gdf =gdf.dropna(axis=0)
print(gdf)
xLoc = 'X.csv'
xdf = pd.read_csv(xLoc)
print(xdf)
xnweLoc = 'X-NWE.csv'
xnweLocdf = pd.read_csv(xnweLoc)
xnwedf =xnweLocdf.fillna(0)
print(xnwedf)
yloc = 'Y.csv'
ydf= pd.read_csv(yloc)
ytranspose = ydf.T
log_ytrans = ytranspose.map(lambda x: np.log(x) if x > 0 else np.nan)
print("log: ", log_ytrans)
loggama = np.dot(xnwedf, log_ytrans.values)
gama = np.exp(loggama)
print(gama)
np.savetxt('gama.csv', gama, delimiter=',', header='Result', comments='')
```

Figure 3.13: codes of calculating thermal conductivity

Material	From Literature Review				Directly measured					UNIPD-Cheap GSHPs database		
	λ, W m^{-1} K^{-1}		ρ c_p, MJ m^{-3} K^{-1}	ρ, in 10^3 Kg m^{-3}	λ, W m^{-1} K^{-1}			ρ c_p, MJ m^{-3} K^{-1}	ρ, in 10^3 Kg m^{-3}	λ, W m^{-1} K^{-1}		
	min	*max*	[a]	[a]	*min*	*max*	*REC*			*min*	*max*	*rec.*
Sedimentary rocks	0.59	7.70			1.03	5.62				**0.59**	**7.70**	
conglomerate	1.50	5.10	*1.8-2.6*	*2.2-2.7*						**1.50**	**5.10**	**1.94**
sandstone	0.72	6.50	*1.8-2.6*	*2.2-2.7*	1.03	4.54	2.00	2.06-2.28	2.43-2.66	**0.72**	**6.50**	**2.60**
clay-mudstone	0.59	3.48	*2.1-2.4*	*2.4-2.6*	1.47	3.21	2.54	1.80-2.23	2.70	**0.59**	**3.48**	**2.13**
limestone	0.60	5.01	*2.1-2.4*	*2.4-2.7*	2.42	4.41	2.88	1.81-2.22	2.35-2.80	**0.60**	**5.01**	**2.50**
dolomite	0.61	5.73	*2.1-2.4*	*2.4-2.7*	1.96	5.22	3.65	2.03-2.34	2.47-2.78	**0.61**	**5.73**	**3.58**
marlstone	1.78	2.90	*2.2-2.3*	*2.3-2.6*						**1.78**	**2.90**	**2.04**
gypsum	1.15	2.80	*2.0*	*2.2-2.4*						**1.15**	**2.80**	**1.60**
anhydrite	1.50	7.70	*2.0*	*2.8-3.0*						**1.50**	**7.70**	**4.77**
Igneous rocks	0.44	5.86			0.86	3.29				**0.44**	**5.86**	
granite	1.49	4.45	*2.1-3.0*	*2.4-3.0*	2.02	3.68	3.13	1.80-2.12	2.66-2.73	**1.49**	**4.45**	**2.74**
diorite	1.38	4.14	*2.9*	*2.9-3.0*	1.99	3.04	2.50	1.75-2.10	2.60-2.71	**1.38**	**4.14**	**2.40**
syenite	1.35	5.20	*2.4*	*2.5-3.0*	2.20	2.66	2.41	2.02-2.06	2.69	**1.35**	**5.20**	**2.51**
gabbro	1.52	5.86	*2.6*	*2.8-3.1*	2.41	2.79	2.60	2.08-2.04	2.84	**1.52**	**5.86**	**2.41**
rhyolite	1.77	3.98	*2.1*	*2.6*	1.89	3.29	2.61	1.95-2.09	2.11-2.5	**1.77**	**3.98**	**2.96**
dacite	2.00	3.91	*2.9*	*2.9-3.0*						**2.00**	**3.91**	**2.60**
andesite	0.64	4.86	*2.3-2.6*	*2.6-3.2*	0.96	1.39	1.16	1.38-1.57		**0.64**	**4.86**	**1.43**
trachyte	2.20	3.40	*2.1*	*2.6*	1.86	1.95	1.91	1.87-2.00	2.33-2.63	**1.86**	**3.40**	**2.48**
basalt	0.44	5.33	*2.3-2.6*	*2.6-3.2*	0.86	2.69	1.78	1.89-2.07	2.13-3.02	**0.44**	**5.33**	**1.82**
tuff/tuffstone	1.10	2.59								**1.10**	**2.59**	**1.10**
Metamorphic rocks	0.65	8.15			1.98	4.43				**0.65**	**8.15**	
quartzite schist	1.89	8.15	*2.1*	*2.5-2.7*						**1.89**	**8.15**	**5.18**
micaschist	0.65	5.43	*2.2-2.4*	*2.4-2.7*	1.98	4.43	2.83	2.09-2.26	2.72-2.76	**0.65**	**5.43**	**2.53**
gneiss	0.84	4.86	*1.8-2.4*	*2.4-2.7*	3.04	3.89	3.70	2.19 - 2.2	3.03	**0.84**	**4.86**	**2.95**
phyllite	1.50	3.33			1.45	2.94	2.59	1.41-1.95	2.76-2.82	**1.45**	**3.33**	**2.45**
amphibolite	1.35	3.90	*2.0-2.3*	*2.6-2.9*						**1.35**	**3.90**	**2.90**
serpentinite	2.41	4.76			2.01	3.72	2.62	2.1-2.2	2.63-2.82	**2.01**	**4.76**	**2.52**
marble	0.98	5.98	*2.0*	*2.5-2.8*						**0.98**	**5.98**	**2.50**
nconsolidated sediments												
clean gravel, dry	0.13	0.9	*1.3-1.6*	*1.8-2.2*	0.14	0.55	0.33			**0.14**	**0.9**	**0.4**
heterometric gravel with sand, wet	0.18	3.00			0.94	1.33	1.08			**0.2**	**3.00**	**1.08**

Figure 3.14: Table of recommended thermal conductivity values[7]

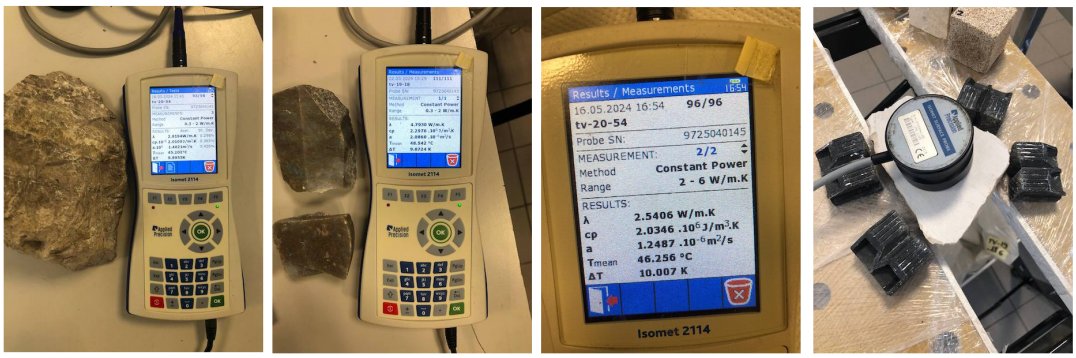

(a) (b) (c) (d)

Figure 3.15: In this figure (a) represents Dolomite,(b) Anhydrite, (c) and (d) Limestone

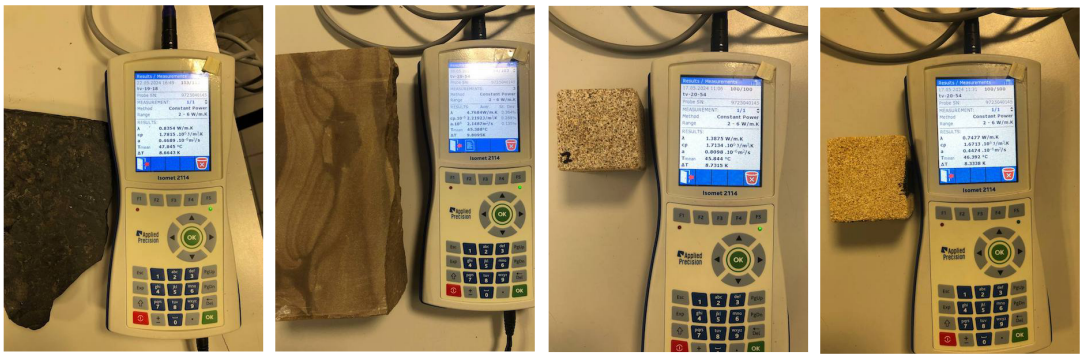

Figure 3.16: In this figure (a) represents Organic Shale, (b) sandstone, (c) sandstone with high porosity, and (d) organic sandstone)

Sample	Dolomite	Sandstone	Organic sand	Anhydrite	Organic shale	lime stone
TC(W/m.k)	2.819	4.74	0.7477	4.793	0.8354	2.5406

Figure 3.17: Thermal Conductivity measured in Lab

steady-state measurement methods. The built-in menu system on color graphic display and the alphanumeric keypad enable effective interactive communication with the device. Measurement data are stored in the high-capacity internal memory. The content of the memory is accessible through the display or can be transferred to a PC through a USB port. Calibration data in internal memory ensures the interchangeability of probes without affecting the accuracy of the measurement. The supplied software package enables the updating of calibration coefficients after recalibration of measurement probes through reference materials. The device can be powered from mains or internal rechargeable batteries at outdoor, in situ measurements.(Figure3.18)

3.4.3 SAMPLES

In figure3.17, the thermal conductivity of each sample is measured with ISOMET 2114. The thermal conductivity values for each type of rock are calculated using a specific formula, and these calculated values are verified.Figure3.19 compares the mea-

Figure 3.18: ISOMET 2114

Sample	Anhydrite	Dolomite	Limestone	Sandstone	shale
TC measured	4.7	2.82	2.54	4.7	0.89
TC Calculated	3.9	3.1	2.61	2.2	1.6

Figure 3.19: Table of the thermal conductivity measured and calculated.

sured values from the lab with the values calculated using the formula, and the results are deemed acceptable.

In Figure3.19, the thermal conductivity of the sandstone in our calculation is decreased because the sandstone contains an oil reservoir, and the fluid content affects thermal conductivity. As we know, oil can reduce thermal conductivity. In Chapter 4, I explained more about the parameters affecting thermal conductivity.

3.5 Artificial Neural Network

I calculated the thermal conductivity using a formula and verified it with the measured thermal conductivity in the laboratory. I can use this thermal conductivity to apply Neural Networks in my predictions.

3.5.1 Geolog's Step-by-Step Process for Predicting Thermal Conductivity

Data Selection and Preparation

For data input, the following logs are selected (Figure3.20(c)):

- CGR (Compensated Gamma Ray)
- Neutron Porosity (Nphi)
- Density
- Resistivity
- Total Porosity
- Sonic Log

An associated log represents the output of a previously calculated thermal conductivity.

Architecture of an ANN

- input Layer: The input layer contains six neurons, each corresponding to one of the selected logs.
- Hidden Layer: A single hidden layer with 2 neurons was specified. This hidden layer processes the inputs using a non-linear activation function, which assists the network in learning complex relationships.(Figure3.21)
- Output Layer: The output layer is one neuron that outputs the predicted thermal conductivity.

Training the ANN

- Initialization: The network's weights and biases are initialized, which can be done randomly or using specific methods such as Xavier or He initialization.(Figure3.20(b))

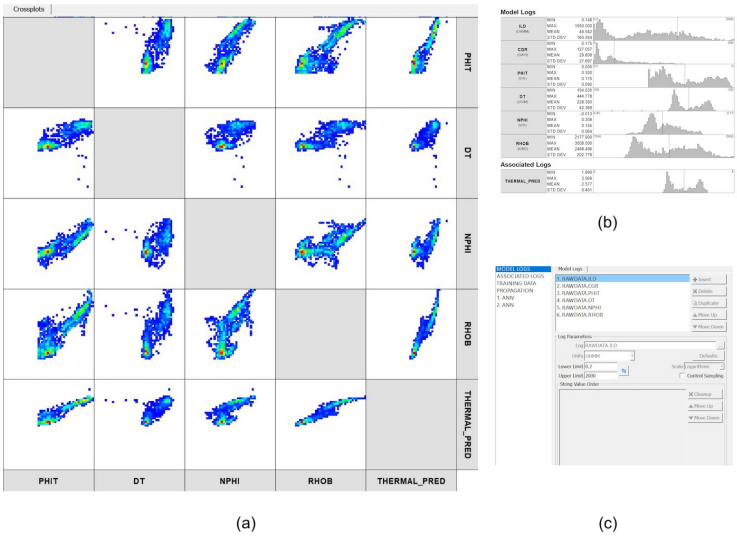

Figure 3.20: Model Logs

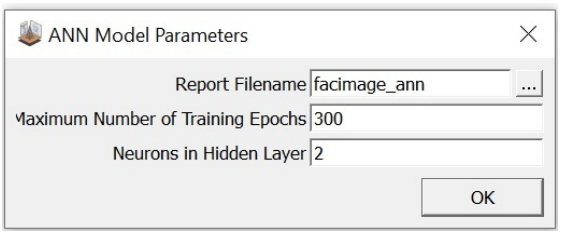

Figure 3.21: Logs ANN Model Parameters

- During forward propagation, for each epoch
- The input data is fed into the network.
- Each input value is multiplied by its corresponding weights and summed in the hidden layer neurons.
- An activation function is applied to the weighted sums.
- The outputs from the hidden layer are then passed to the output layer neuron, which produces the predicted thermal conductivity.
- Backpropagation: The error is propagated back through the network to update the weights. This is done using an optimization algorithm like gradient descent, which adjusts the weights to minimize the error.
- Epochs: This process is repeated for the maximum number of epochs (300 in my case), continually refining the weights to improve prediction accuracy.(Figure3.21)

Propagation of the Model

- Once the ANN is trained, the next step is to use this trained model to predict thermal conductivity for the entire well.
- Propagation: The trained ANN model takes input logs from all depth intervals of the well and predicts the thermal conductivity for each depth interval.(Figure3.20(a))

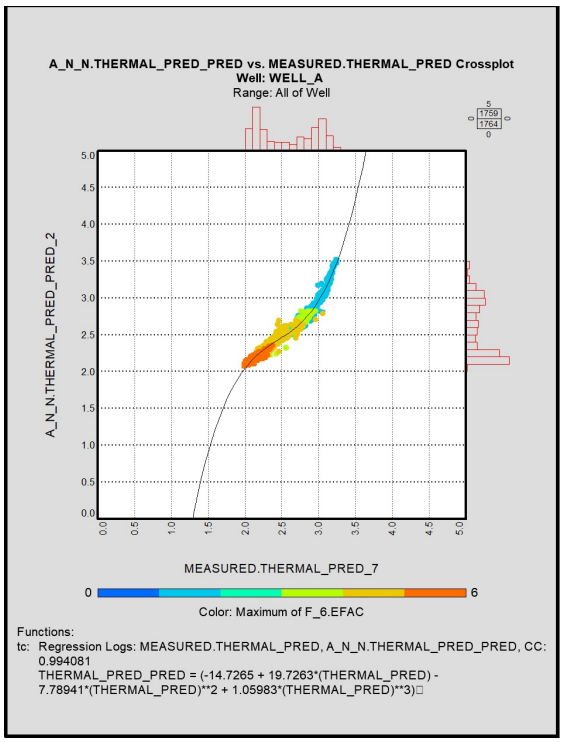

Figure 3.22: Cross-plot of ANN-Predicted TC vs Measured TC

3.6 Validation of ANN Predictions Against Measured Thermal Conductivity Values

After using the ANN approach to predict thermal conductivity in the first well, I validated the results by creating a cross-plot and running a regression analysis with the measured thermal conductivity data. The relationship between the predicted and measured values is depicted in the figure3.22, and the correlation coefficient (CC) is over 95%, indicating that our prediction is accurate. To gain a deeper understanding, I categorized the data into 6 clusters, each representing different lithology properties and porosity properties. I used different colors to represent the clusters, as shown in the figure3.23. Blue is associated with low porosity and high density, while red and orange are associated with high porosity and low density.

3.7 Values predicted vs. values calculated

I determined the Mean Absolute Error (MAE), Mean Squared Error (MSE), and R-squared (Rš) using Python. Figure3.25 displays predicted and calculated thermal conductivity values to illustrate the model's performance.

3.7.1 Explanation of Performance Metrics

- Mean Absolute Error (MAE): An average of the absolute differences between predicted and actual values, providing a straightforward measure of prediction accuracy. The low MAE(0.032) indicates that, on average, the model's predictions are very close to the actual measurements.

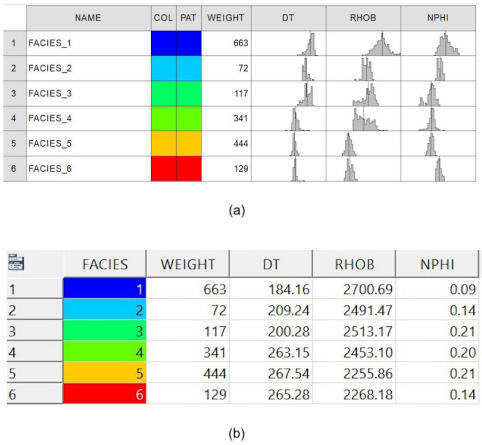

	NAME	COL	PAT	WEIGHT	DT	RHOB	NPHI
1	FACIES_1			663			
2	FACIES_2			72			
3	FACIES_3			117			
4	FACIES_4			341			
5	FACIES_5			444			
6	FACIES_6			129			

(a)

	FACIES	WEIGHT	DT	RHOB	NPHI
1	1	663	184.16	2700.69	0.09
2	2	72	209.24	2491.47	0.14
3	3	117	200.28	2513.17	0.21
4	4	341	263.15	2453.10	0.20
5	5	444	267.54	2255.86	0.21
6	6	129	265.28	2268.18	0.14

(b)

Figure 3.23: Legend of Clusters with histograms(a) and wights (b)

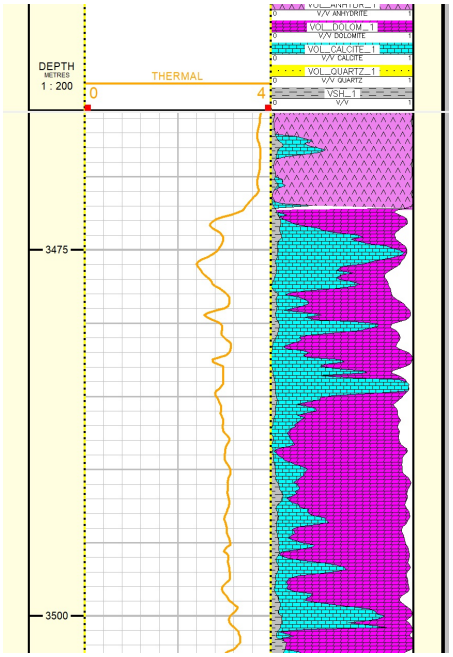

Figure 3.24: Layout of Thermal conductivity Predicted using ANN approach

Depth (m)	Predicted Thermal Conductivity (ANN) (W/m·K)	Calculated Thermal Conductivity (W/m·K)	Absolute Error (W/m·K)
3500.9328	3.185124	3.123426	0.061698
3501.0852	3.144276	3.039373	0.104903
3501.2376	3.140886	2.985538	0.155348
3501.3922	3.170865	3.148997	0.021868
3501.5424	3.186992	3.168432	0.01856
3501.6948	3.195192	3.181779	0.013413
3501.8472	3.194873	3.179503	0.01537
3501.9996	3.178885	3.157304	0.021581
3502.1521	3.121519	3.102731	0.018788
3502.3044	3.042074	3.039616	0.002458

Figure 3.25: Calculated and predicted thermal conductivity values

- Mean Squared Error (MSE): The average of the squared differences between predicted and actual values. This metric emphasizes larger errors due to the squaring process, and the low MSE(0.0018) value indicates that such large errors are rare, confirming the model's precision.
- R-squared (R^2): A statistical measure of how well the predicted values approximate the data. The Rš value of 0.98 indicates that nearly all variability in the actual thermal conductivity values is captured by the model's predictions, underscoring its high reliability

The ANN model performs exceptionally well at predicting thermal conductivity, with a Mean Absolute Error (MAE) of 0.032 and a Mean Squared Error (MSE) of 0.0018. These low error values indicate that the model's predictions are very close to the actual values, on average. Additionally, the R-squared (R^2) value of 0.98 suggests that the predictions made by the model account for 98% of the variance in the calculated thermal conductivity values. This high Rš value signifies a strong correlation between the predicted and actual values, indicating that the model explains almost all the data variability. The depth values provide context for where the thermal conductivity measurements were taken, showing consistency across a range of depths. The small absolute errors between the predicted and calculated thermal conductivity across these depths further emphasize the model's accuracy. These metrics illustrate the model's reliability and effectiveness in predicting thermal conductivity in geological studies, making it a valuable tool for researchers in this field.

3.8 Propagation Of the ANN model in the other wells

After evaluating the model performance and achieving a 98% correlation coefficient, the model is ready to be applied to other wells to predict thermal conductivity. Since thermal conductivity data is unavailable for these other wells, I used N-fold cross-validation to validate my model. This method ensures that the model's predictions are reliable and accurate despite the absence of direct thermal conductivity measurements in the new wells. The results and a comprehensive analysis of these findings will be presented in the next chapter. This section will provide detailed interpretations of the relationship between thermal conductivity and various petrophysical properties. By examining these correlations, we will gain valuable insights into how thermal conductivity interacts with and is influenced by factors such as porosity, permeability, and mineral composition. These insights will validate the model's predictions and enhance our

understanding of the subsurface geological conditions, contributing to more informed decisions in geophysical exploration and resource management.

4

Results

4.1 Overview

This chapter presents findings from my study predicting ground thermal conductivity using neural networks trained on well-log data. This study aims to evaluate the effectiveness of machine learning techniques in estimating key thermal parameters in subsurface environments, such as thermal conductivity. I begin Chapter 4 by providing an overview of the dataset. It consists of well-log data collected from various geological formations in a particular geographic area. The parameters included in the dataset are gamma-ray measurements, resistivity, temperature, and other relevant information. To train the models, I describe the layers, activation functions, and optimization algorithms used in our neural network architecture. My discussion also includes data cleaning, normalization, and feature engineering techniques designed to enhance the predictive performance of my models. We evaluate the performance of the trained neural networks in predicting ground thermal properties. To assess the accuracy and reliability of predictions, I use quantitative metrics. Models that capture underlying relationships between input features and thermal properties can be evaluated using cross-plots comparing predicted values with ground truth measurements.

4.2 Analysis of thermal conductivity

In this section, I utilized layouts, cross-plots, and a histogram to analyze wells from the first oil field. Similar to the previous chapter, this field's lithology is diverse and includes anhydrite, dolomite, limestone, sandstone, and shale.

Based on the clusters of well-1, each cluster color represents a specific lithology with a corresponding porosity percentage. The porosity increases from the blue cluster to the red one, decreasing thermal conductivity. This is due to the inverse relationship between porosity and thermal conductivity.

To validate my result, I calculated the Mean Absolute Error, Mean Squared Error, and R-squared (predicted vs. calculated).

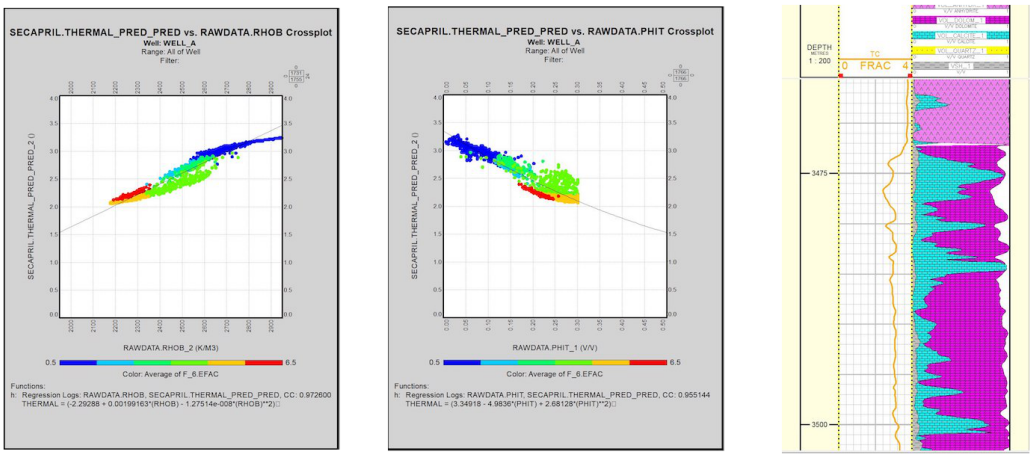

Figure 4.1: (a) Cross-plot of TC and Denisty, (b) Cross-plot of TC and Totol Porosity, (c) layout of lithology and TC curve in well-1 of the First oil field

4.2.1 First oil field

I predicted thermal conductivity in this oil field and then validated the result for two wells. I used cross-plots to demonstrate the relationship between thermal conductivity and density. A regression analysis was used to show the correlation coefficient with an equation.

well-1

In Figure4.1(a), the cross-plot displays the predicted thermal conductivity and density log in well-1, with colors representing clusters from the previous chapter. The clusters range from high to low porosity (orange and red clusters indicate low density, while blue indicates high density). As observed in the cross-plot, the thermal conductivity increases as the density increases, indicating a direct relationship between the two. This supports the accuracy of my prediction.

Regarding lithology and porosity, the blue area indicates higher density than other areas, and it is associated with Anhydrite, which has high thermal conductivity. The red and orange areas are related to sandstone (2.6 g/cc) and shale (2.2 g/cc) due to their high porosity and low density, while the blue area is related to Anhydrite (2.98 g/cc) and Dolomite (2.87 g/cc).

The correlation coefficient is 97%.

The equation is given by:

$$TC = -2.29 + 0.0019\rho - 1.27 \times 10^{-8}\rho^2$$

The next graph(figure4.1(b)) illustrates the predicted thermal conductivity versus total porosity. The x-axis represents porosity, while the y-axis represents TC. I used color to group the data based on porosity and lithology. The color gradient ranges from blue to red, with an increase in porosity.

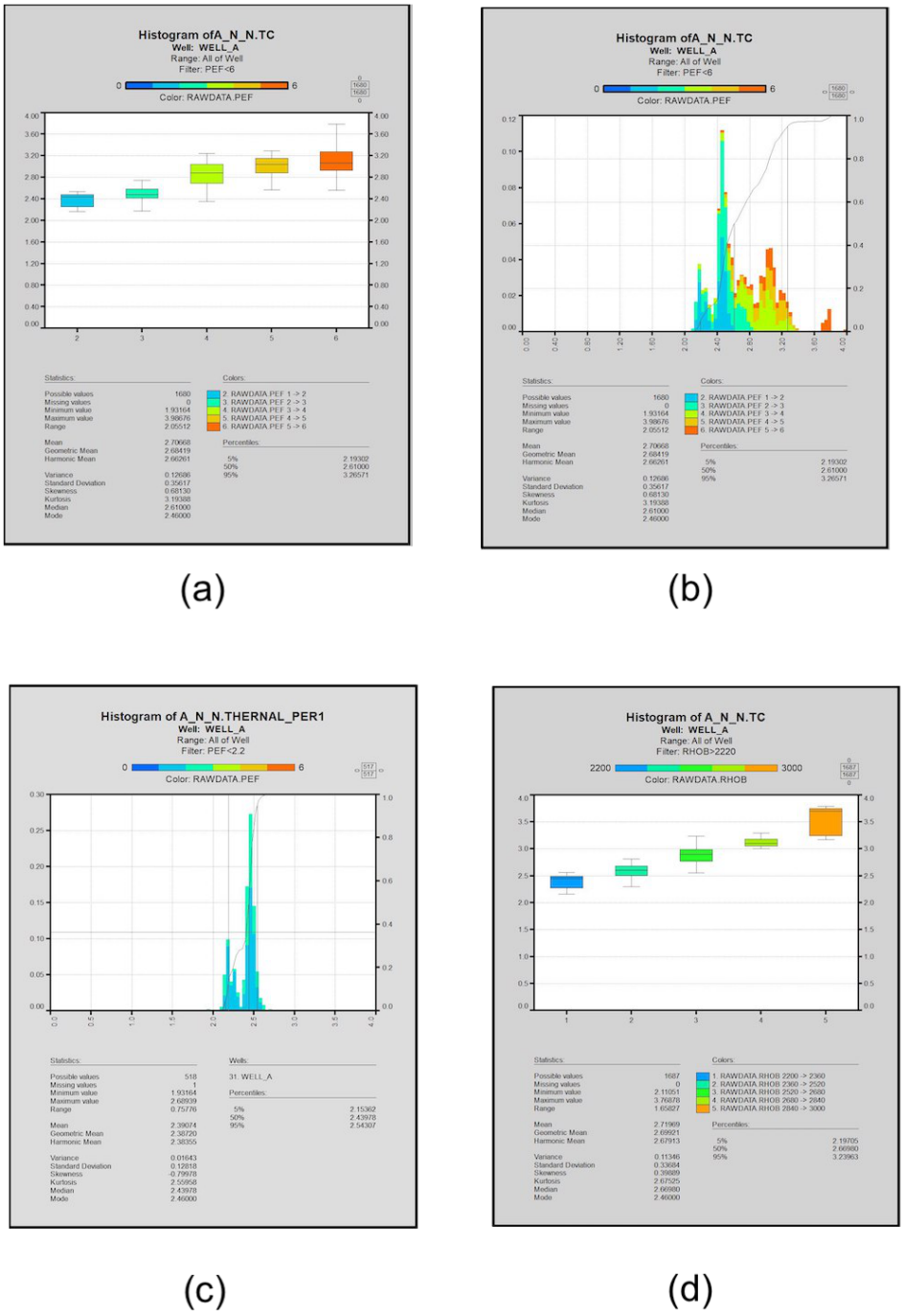

Figure 4.2: (a)Histogram of TC (box chart) (b) Histogram of TC (bar chart), (c) histogram of TC in sandstone zone colored by PEF (d) Histogram of TC cored by Density log in well-1 of First oil field. The color bar range increases from blue to orange

We can observe (figure4.1(b))that high porosity is represented by the red and orange clusters (20% to 30%), while low porosity is indicated by the blue area (1% to 0). Consequently, there is an inverse relationship between porosity and thermal conductivity. As porosity increases, the thermal conductivity decreases. Anhydrite and dolomite exhibit the highest TC, whereas shale has the lowest TC relative to porosity. The correlation coefficient is 95%. The equation is given by:

$$TC = 3.34 - 4.98\Phi + 2.68\Phi^2$$

The following graph(figure4.1(c))shows the curve of TC (Thermal conductivity) and the lithology track. At the top of the track, the lithology consists of anhydrite. As we move downward, we encounter layers of dolomite intermixed with limestone, which can be referred to as dolomitic limestone. The thermal conductivity of Anhydrite ranges from 3.7 to 3.9, while limestone ranges from 2.6 to 2.8, and dolomite ranges from 2.9 to 3.3.

In figure 4.2I created several thermal conductivity (TC) histograms using different styles. The first(a) is a box chart showing the frequency of TC in well-1. I used the Photoelectric Factor log (PEF) to understand better because PEF can determine lithology. Based on the PEF log values, each color represents a different lithology: blue for shale, green for sandstone, light green for limestone, yellow for dolomite, and orange for anhydrite. From left to right, thermal conductivity increases.

The bar chart histogram(b) displays the range of values for different lithologies, with shale having a minimum value of 1.9 and anhydrite having a maximum value of 3.9. The colors in the chart correspond to the lithology categories described in the first histogram.

To demonstrate the impact of hydrocarbons on TC, I utilized a histogram(c) and applied a filter for PEF log values smaller than 2.2, highlighting sandstone. In the resulting bar chart, two sections of sandstone are visible in the same color but with varying thermal conductivities. The first section exhibits lower TC than the second section, attributed to the presence of hydrocarbons in this area, indicating that hydrocarbons can reduce TC. The last histogram(d) shows the frequency of TC, colored by density from blue to orange. As density increases, TC also increases, demonstrating a better understanding of the relation between TC and density.

well-2

The figure4.3 shows the cross-plot validation of predicted TC by the N-fold method. This means I validated it by training 25% of the data and then obtained the ANN model. After that, I tested the model with the rest of the data, and it performed well, showing a 97% correlation coefficient. I also determined the mean absolute error (0.43) and mean squared error (0.003).

The cross-plot of TC and density(a) shows that as density increases, TC also increases. The color change from blue to orange on the density log indicates increasing density. There is also a direct relationship between TC and porosity. The correlation coefficient is approximately 98%.Figure4.4(a)

The cross-plot (Figure4.4)(b) of the TC and Sonic logs shows an inverse relationship because the Sonic log measures transition time and not velocity. If transition time increases, TC decreases. The color shows the Sonic log(DT) range increasing from blue

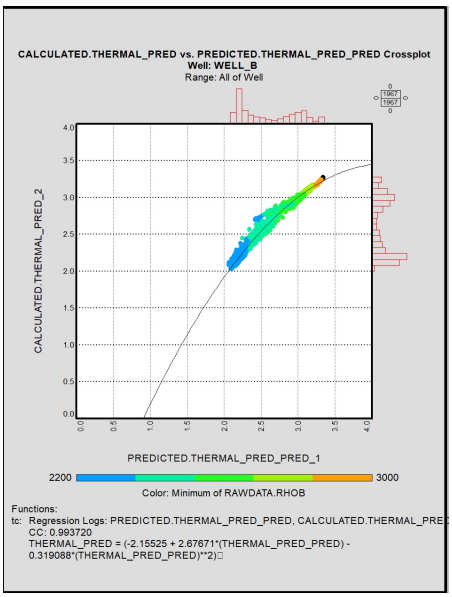

Figure 4.3: Cross plot of TC Predicted and TC Calculated well 2 in the first oil field

to red, and the Correlation Coefficient is about 94%.

The equation is given by:

TC=4.65 - 0.0091*DT

This histogram (box chart) displays the frequency of thermal conductivity in well 2. I used a color gradient to represent the density of the data. The color bar ranges from blue to orange, indicating increasing density. It illustrates that lower thermal conductivity values are represented by the color blue, indicating lower density, while the highest values are represented by the color orange, indicating higher density.(Figure4.4(c))

The following bar chart of figure 4.4(d) represents TC, and I also used a Neutron porosity log to display the porosity. The color of the bar changes from blue to red, indicating that blue represents the highest TC and red represents the lowest TC.4.4(d)

In this histogram of Figure4.5(a), we can observe the frequency of TC in well-2, with density represented by colors ranging from blue to orange. The blue area indicates the lowest Tc values, while the orange area represents the highest Tc values. This is because there is a direct relationship between TC and density. and the last graph(b) shows the curve of TC in well-2.Figure4.5(b)

In this oil field, the Bottom log interval temperature is about 115 in the 3800 m depth, and the mean value of thermal conductivity is 2.7 $W/m \cdot K$, so this oil field could be possible for geothermal purposes regarding properties such as TC, Temperature, water-saturated (45%) and high permeability of reservoir rock(sandstone) and presence of fractures in carbonates and it is good for mide geothermal system

4.2.2 Geothermal Potential Assessment

Several factors need to be considered to assess the potential of an oil field for geothermal purposes, including temperature, thermal conductivity, water saturation, and the suitability for a mid-range geothermal system.

- A temperature of 115 C at a depth of 3800 meters is suitable for a mid-range geothermal system. Geothermal energy typically requires temperatures above

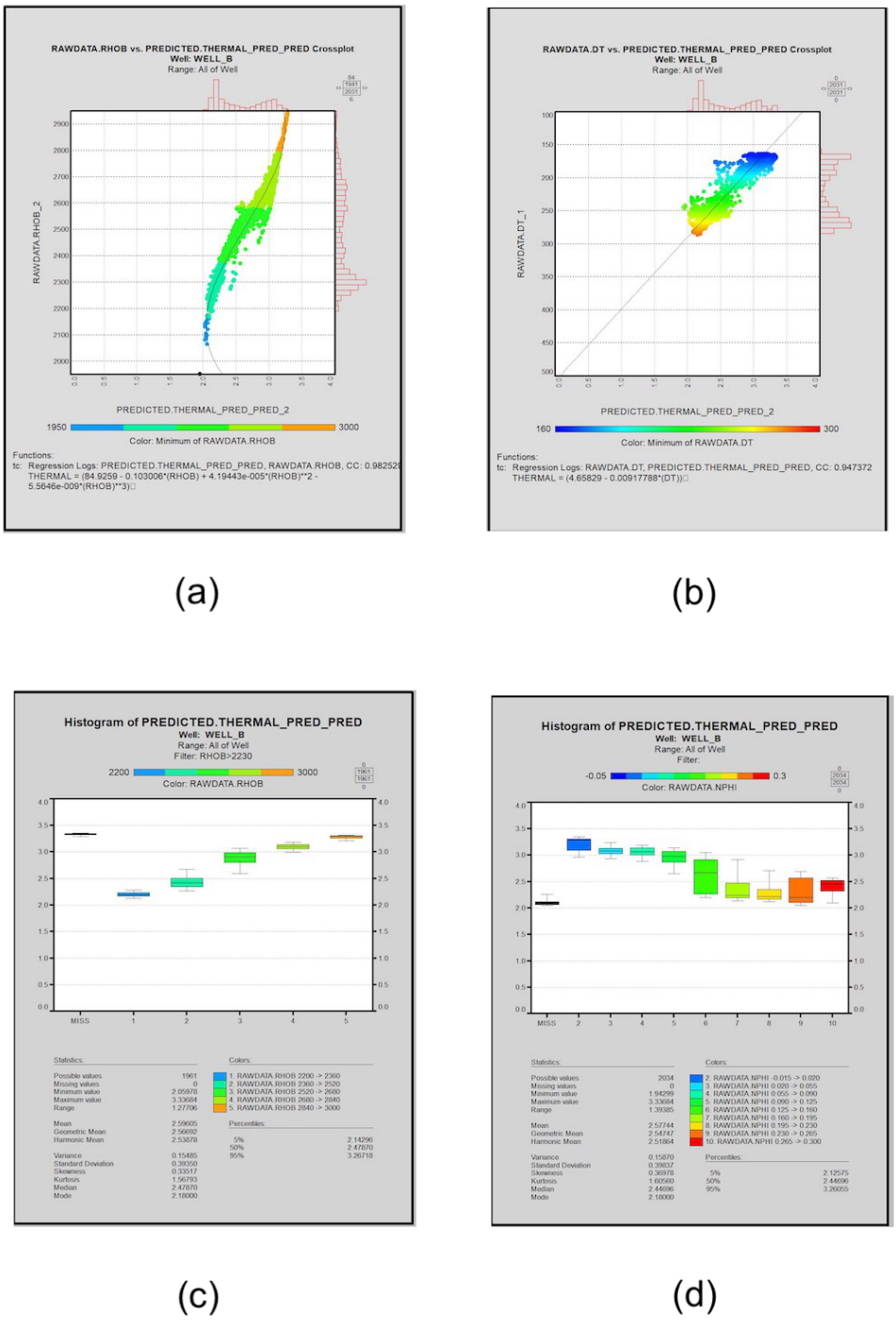

Figure 4.4: (a) Cross-plot of TC and Density log(colored by density, (b) Cross plot of TC and Sonic colored by DT (c) Histogram of TC colored bt Density (d) histogram of TC colored by Neutron porosity

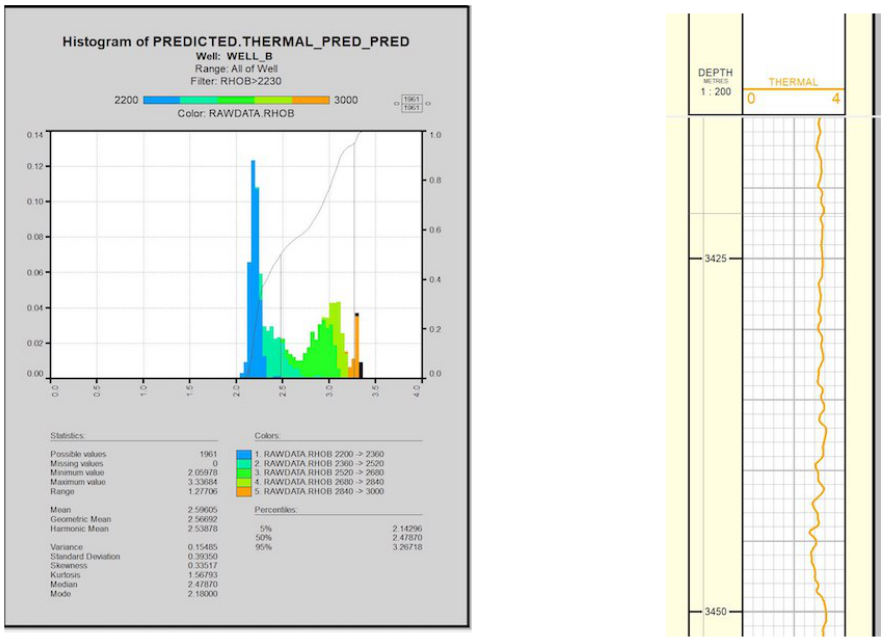

(a) (b)

Figure 4.5: (a)Histogram Of TC colored bt Density log(RHOB),(b)Represent the TC curve of well-2 in first oil field

100řC, which can support binary cycle power plants commonly used for medium-temperature geothermal resources.

- Thermal conductivity (TC) is crucial as it affects heat transfer efficiency. A mean TC of 2.7 $W/m \cdot K$ is considered good for geothermal purposes. Higher thermal conductivity facilitates better heat transfer from the reservoir to the surface.
- Water saturation of 45% is beneficial because water acts as a heat transfer medium in geothermal reservoirs. Adequate water saturation ensures efficient heat extraction
- At 3800 meters, drilling and operational costs are significant, but the depth also contributes to reaching higher temperatures, enhancing the feasibility of geothermal energy extraction.
- Reservoir Permeability: The permeability of the reservoir rock(sandstone) is another critical factor. High permeability allows for efficient fluid flow(presence of fractures in Carbontes), which geothermal systems need.

  This oil field seems to have the potential to be converted into a geothermal energy production site. Its moderate temperature, favorable thermal conductivity, and sufficient water saturation suit it for mid-temperature geothermal systems or direct-use applications. To confirm this conversion's feasibility and economic viability, further studies, including detailed geological surveys, reservoir assessments, and economic analyses, are recommended.

4.2.3 Second oil field

I utilized the ANN model to predict TC in the second field for 6 wells. The results were validated using N-fold analysis and were found to be acceptable. The correlation coefficient is about 97% figure4.6

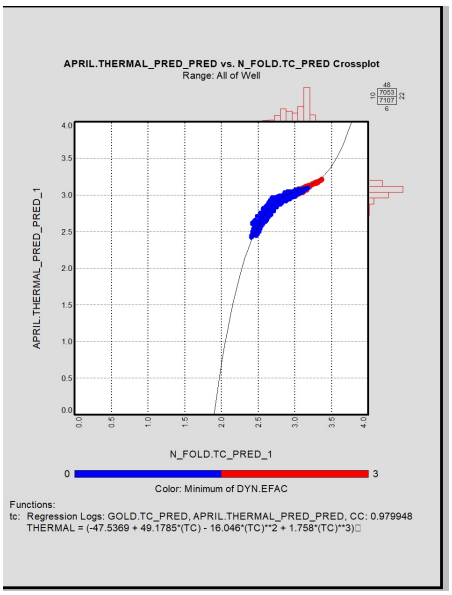

Figure 4.6: Cross-plot of predicted and N-fold method for validation

Well-1

As described in Chapter 3, the lithology of this field primarily consists of limestone with interspersed layers of shale. Therefore, the main mineral composition of this formation is calcite. In Figure4.7(a), the cross-plot of density and TC shows a direct relationship between them. The color bar represents GR and indicates the presence of shale, ranging from blue to red, as GR increases. However, the volume of shale appears to be very low, as indicated by the predominantly blue color. The correlation coefficient is about 96%. The equation is given by:

$$TC = -8.34 + 0.0076\rho - 1.25 \times 10^{-6}\rho^2$$

Figure4.7 (b) shows that the thermal conductivity (TC) histogram ranges from 2.5 to 3.2. The data has been clustered using sonic, density, and neutron logs into two distinct groups based on porosity. The blue cluster, which has low thermal conductivity, represents high porosity, while the red cluster, which has high thermal conductivity, indicates low or zero porosity.

In the figure 4.7(c), the first track shows the TC (orange) and Neutron porosity log (red). The second track displays clusters in well 1, where red represents low porosity and blue represents higher porosity. The last track demonstrates the lithology of the formation, which is limestone. Upon examining the TC and NPHI logs, we notice that as NPHI increases, TC decreases (to 2.4) and vice versa. TC remains almost constant at about 2.9 in the remaining part of the formation due to the pure limestone lithology without any porosity.

Well-2

"The lithology of this well is almost dolomite. Figure 4.8(a) shows the predicted cross-plot of density vs. TC. As can be seen, the x-axis represents TC, and the y-axis represents density. Data points are colored by the photoelectric factor (PEF) log, and almost all data points are orange. This indicates that the PEF range is between 5 to 5.5, related to limestone. Moreover, there is a direct relationship between TC and density. Notably, there is a direct correlation between TC and density. The correlation coefficient is about 98%.

$$TC = -12.4 + 0.01\rho - 1.89 \times 10^{-6}\rho^2$$

The figure4.8 (b)and (c)shows two histograms of thermal conductivity (TC) represented by a bar chart and a box plot. The data are color-coded based on the neutron porosity log (NPHI) to illustrate the relationship between porosity and thermal conductivity; as the neutron log color changes from blue to red, porosity increases while thermal conductivity decreases. Therefore, the blue area repre-

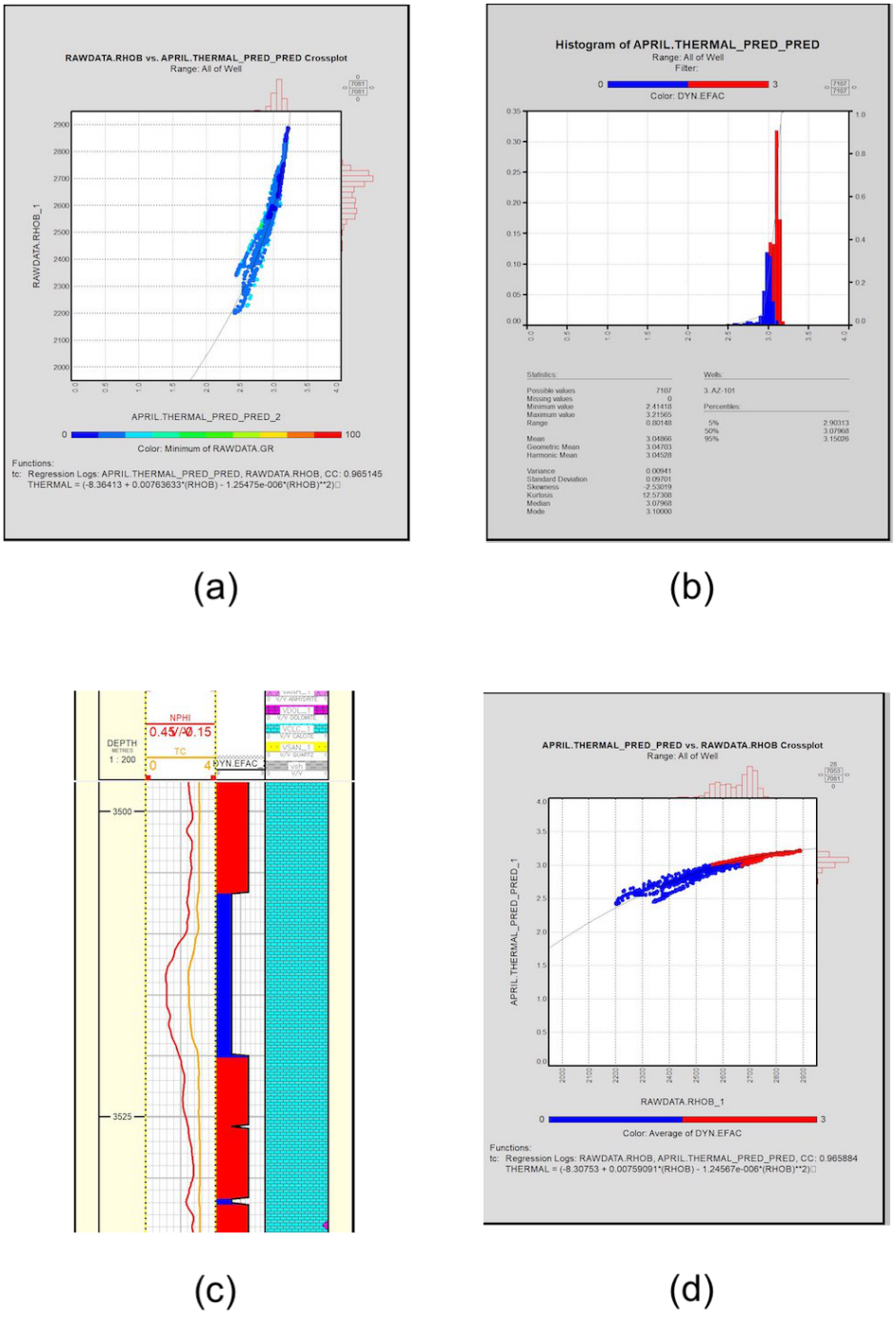

Figure 4.7: (a)Cross-plot of TC predicted and density log colored by GR log, (b)Histogram of TC colored by porosity clustering, (c)TC curve, clusters, and lithology (Limestone), (d)Cross-plot of TC predicted and density log colored by porosity clustering

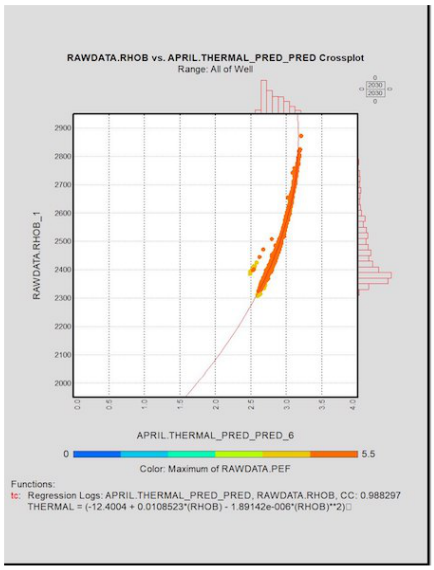

(a)

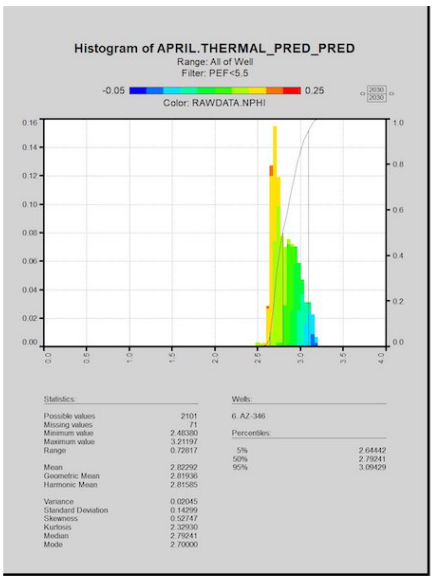

(b)

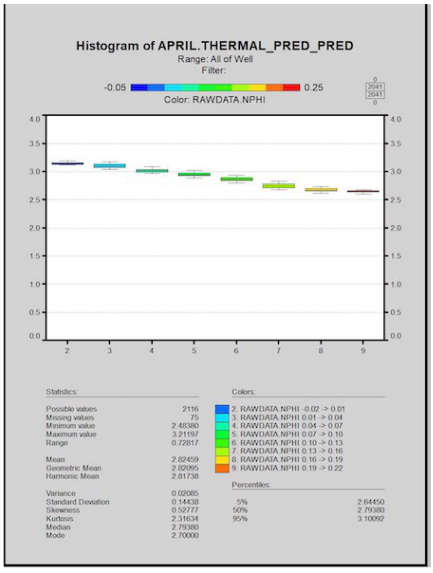

(c)

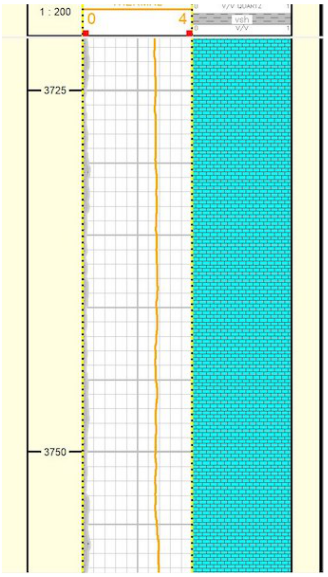

(d)

Figure 4.8: (a)Cross-plot of TC predicted and density log colored by PEF log, (b)Histogram of TC colored by Neutron porosity log, (c)Histogram of TC predicted colored by Neutron porosity log,(d)TC curve, clusters, and lithology (Limestone)

sents low porosity and high thermal conductivity, while the red represents high porosity and low thermal conductivity.

Figure (d)4.8 demonstrates that Well 2's curve and lithology are nearly constant, with a consistent green limestone pattern.

well-3

I selected this well because the mean value of porosity of The formation is 16%, and I wanted to understand the effect of porosity on TC, so I predicted thermal conductivity with data of this well. The figure4.9(a) shows a cross-plot demonstrating the relationship between thermal conductivity on the x-axis and density on the y-axis. The data points are color-coded based on total porosity. The color bar indicates the porosity range from 0 to 20 percent, with blue representing low porosity and red representing high porosity. It's clear from the plot that thermal conductivity has an inverse relationship with porosity. The correlation coefficient is about 95%

The relationship is given:

$$TC = -520 + 6.65\rho - 0.002 \times \rho^2 + 3.78 \times 10^{-8}\rho^3$$

Figure 4.9 (b)and(c) show two types of histograms: a bar chart and a box chart. They show the thermal conductivity frequency and are colored based on total porosity from blue to red to indicate increasing porosity. and the mean value of thermal conductivity is about 1,8 W/můK.

well-4, well-5, well-6

In addition to my previous work, I introduced three new wells to expand the ANN model for predicting thermal conductivity. The results are displayed in the figure4.104.114.12 The scatter plots indicate the relationship between thermal conductivity and density, with colors representing total porosity. It is evident that the porosity of these data points is very low, leading to an increase in thermal conductivity compared to well-3. The histograms show thermal conductivity distribution, with colors indicating total porosity. In this case, blue signifies low porosity, associated with increased thermal conductivity. Total porosity values are 1.2%, 1.4%, and 0.4%, and thermal conductivity (TC) ranges from 2.9 to 3 $W/m \cdot K$.

To evaluate the geothermal potential at a depth of 4200 meters with a bottom hole temperature of 137řC, water saturation of 25%, and thermal conductivity of 2.8 $W/m \cdot K$; considering these factors, it is possible that high geothermal energy could be generated at this location. The thermal conductivity, bottom hole temperature, and depth suggest a significant heat source, and the water saturation could enhance the thermal conductivity and fluid flow. However, further analysis and detailed exploration would be necessary to confirm the geothermal potential and optimize the design of the geothermal system.

4.2.4 Third oil field

In this oil field, lithology included Dolomite, limestone, and some layers of Anhtdrite, and TC is predicted according to the ANN model as same as previous data, and for validation of the results again used the N-fold as explained before in other oil fields.

well-1

In the figure4.13, a cross-plot displays the correlation and validation of the Artificial Neural Network (ANN) model in the first well. The y-axis represents the new prediction utilizing the N-fold method, while the x-axis represents the initial prediction. The correlation coefficient is approximately 98%.

As a result, the results appear to be acceptable.

In this figure4.14(a), the cross-plot of Tc (thermal conductivity) and density shows a direct relationship, with a correlation coefficient of approximately 98%. The color bar is based on total porosity, transitioning from blue to red with increasing values. The blue area represents low levels of porosity and porosity but high Tc, while the

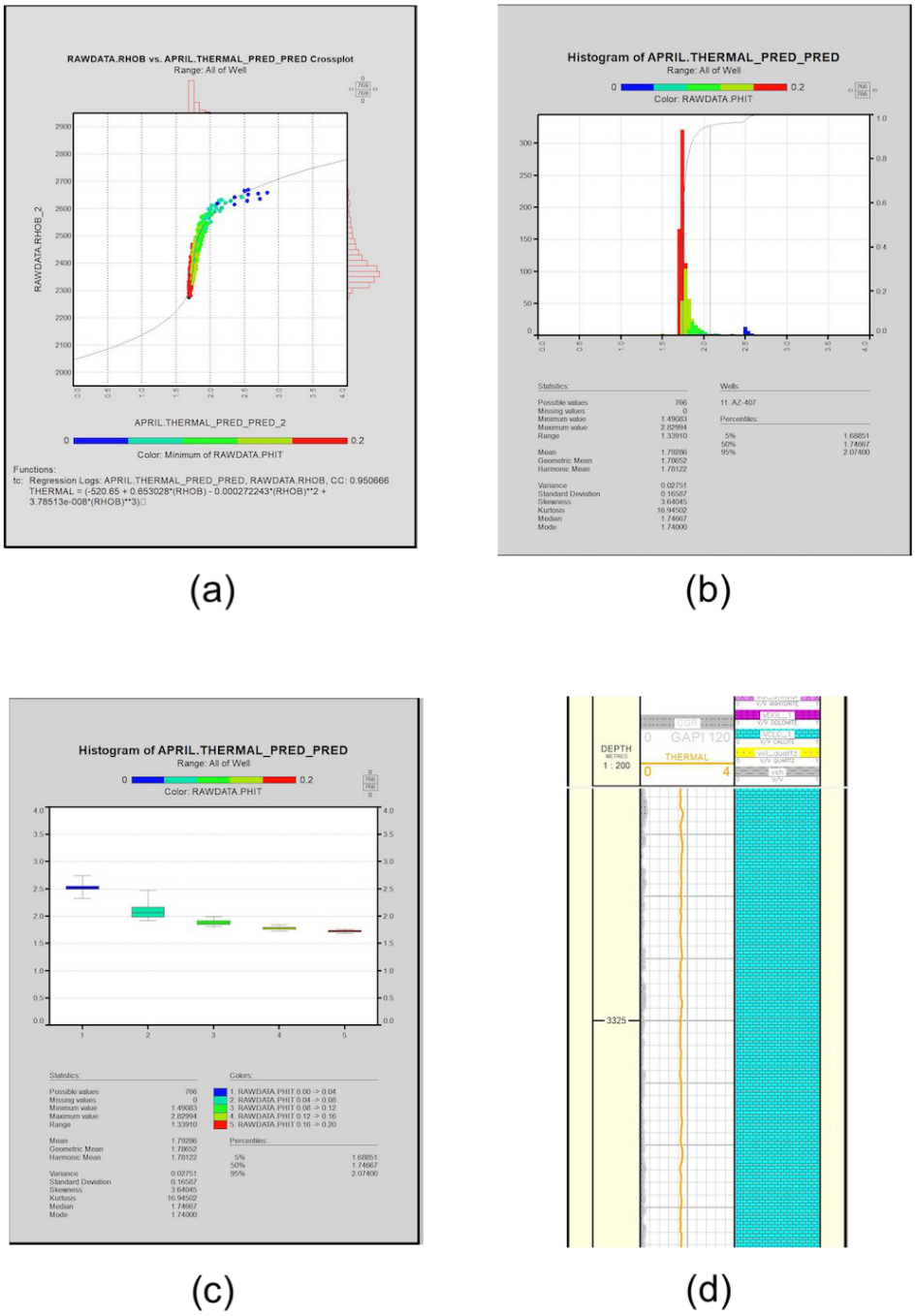

Figure 4.9: (a)Cross-plot of TC predicted and density log colored by Total Porosity, (b)Histogram of TC colored by Total porosity, (c)Histogram of TC predicted colored by Total porosity,(d)TC curve, clusters, and lithology (Limestone)

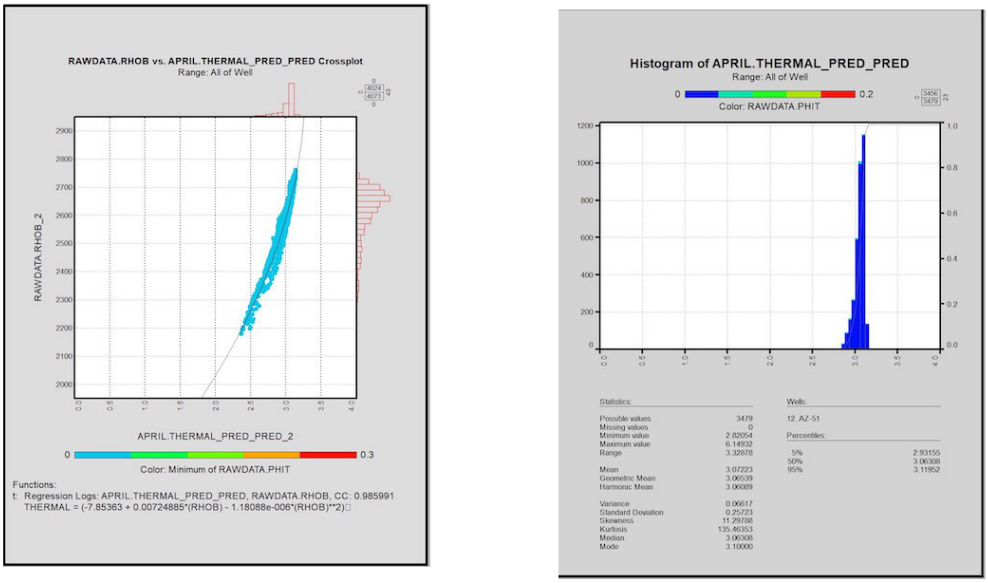

(a) (b)

Figure 4.10: (a)Cross-plot of TC predicted and Density log colored by Total Porosity,(b)Histogram of TC predicted colored by Total Porosity(well-4, The Second field)

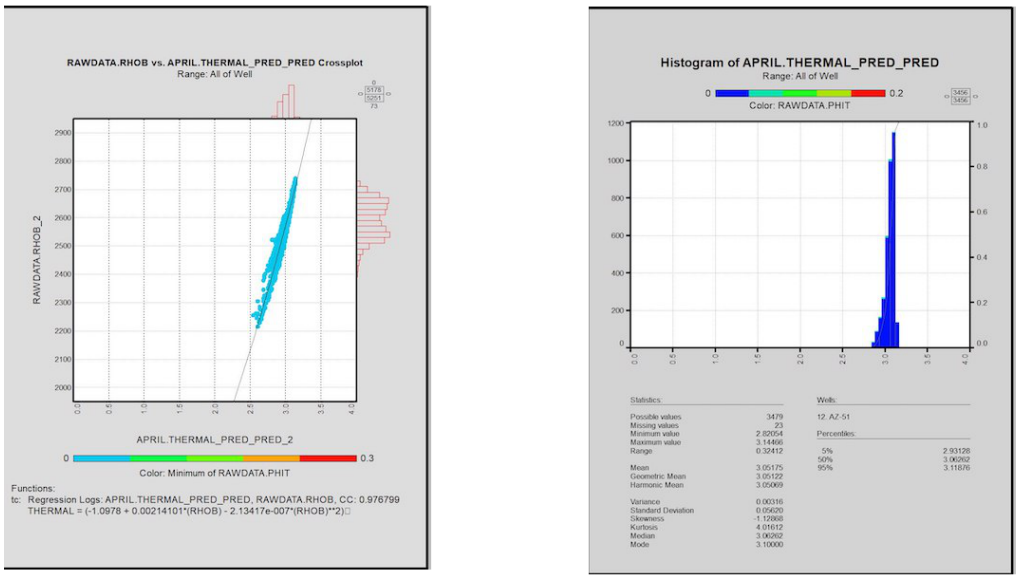

(a) (b)

Figure 4.11: (a)Cross-plot of TC predicted and Density log colored by Total Porosity,(b)Histogram of TC predicted colored by Total Porosity(well-5, The Second field)

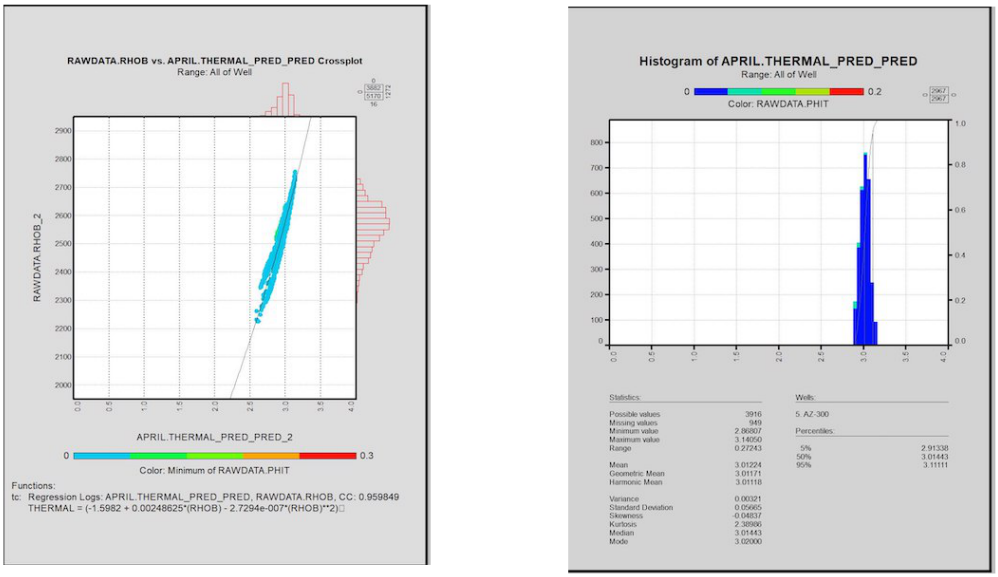

(a) (b)

Figure 4.12: (a)Cross-plot of TC predicted and Density log colored by Total Porosity,(b)Histogram of TC predicted colored by Total Porosity(well-6, The Second field)

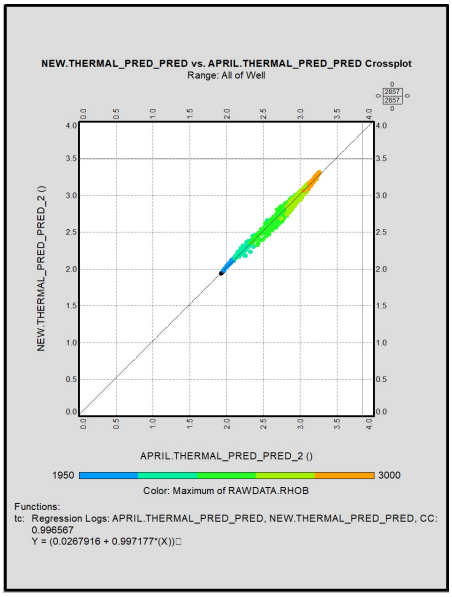

Figure 4.13: Cross-plot of TC predicted and N-fold method for validation The ANN model(well-1, Third oil field)

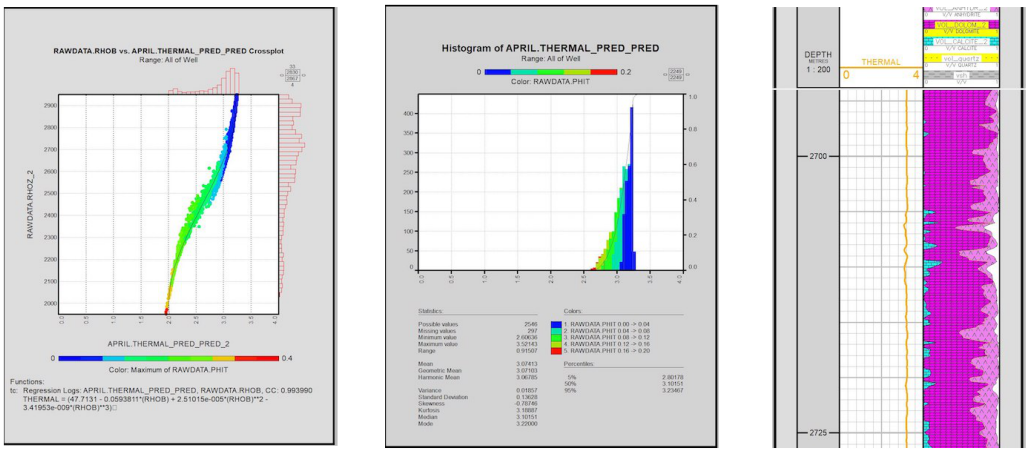

(a) (b) (c)

Figure 4.14: (a)Cross-plot of TC predicted and Density log colored by total porosity,(b)Histogram of TC colored by total porosity, (c) TC curve and lithology track (well-1, Third oil field)

red area indicates the highest porosity with the lowest thermal conductivity. The relationship is as follows:

$$TC = 47 - 0.05\rho + 2.5 \times 10^{-5}\rho^2 - 3.4 \times 10^{-9}\rho^3$$

In Figure 4.14 (b), the histogram (bar chart) of TC in well-1 is shown, with the color bar representing the Neutron porosity log. The blue area represents high TC, indicating low porosity according to the color bar. Track (c) demonstrates the relationship between TC and lithology, including Dolomite, Anhydrite, and limestone layers.

well-2

The artificial neural network (ANN) model is correlated and validated in the second well in the figure labeled Figure4.15 The y-axis represents the new prediction utilizing the N-fold method, while the x-axis represents the original prediction. There is a correlation coefficient of approximately 98%.

In this figure4.16 (a), there is a direct correlation between Tc (thermal conductivity) and density, with a correlation coefficient of approximately 98 percent. With increasing total porosity, the color bar transitions from blue to red. porosity is low in the blue area, but TC is high, whereas the lowest thermal conductivity is found in the red area. Accordingly, the relationship is as follows:

$$TC = 46 - 0.05\rho + 2.4 \times 10^{-5}\rho^2 - 3.3 \times 10^{-9}\rho^3$$

Figure 4.16(b) shows the histogram (bar chart) of TC in well-1, with the color bars representing total porosity logs. According to the color bar, the blue area indicates low porosity due to high TC. TC is correlated with lithology (figure4.16)(c), including the limestone, dolomite, and anhydrite layers.

Based on the parameters of 3300 meters depth, a bottom hole temperature of 105řC, 10% water saturation, thermal conductivity of 2.9 $W/m \cdot K$, and 7% porosity, the site appears to have potential for medium enthalpy geothermal projects. The combination of depth and temperature suggests a significant heat source suitable for binary cycle power plants and direct-use applications. The moderate thermal conductivity would support efficient heat transfer, but the low porosity indicates limited fluid storage capacity. Therefore, techniques like hydraulic fracturing may be needed to enhance permeability. Further detailed studies, including permeability testing, geological surveys, reservoir modeling, and economic feasibility

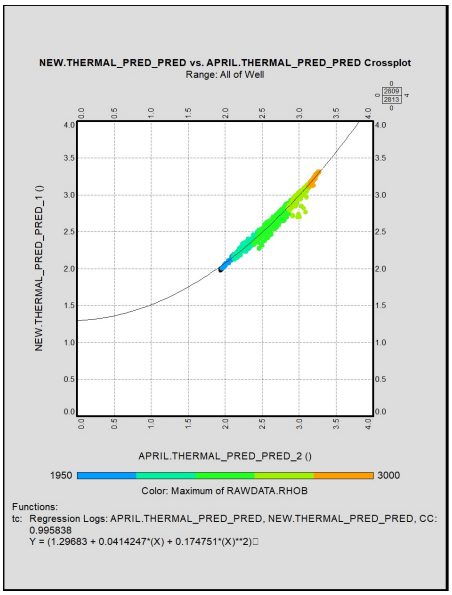

Figure 4.15: Cross-plot of TC predicted and N-fold method for validation The ANN model(well-2, Third oil field)

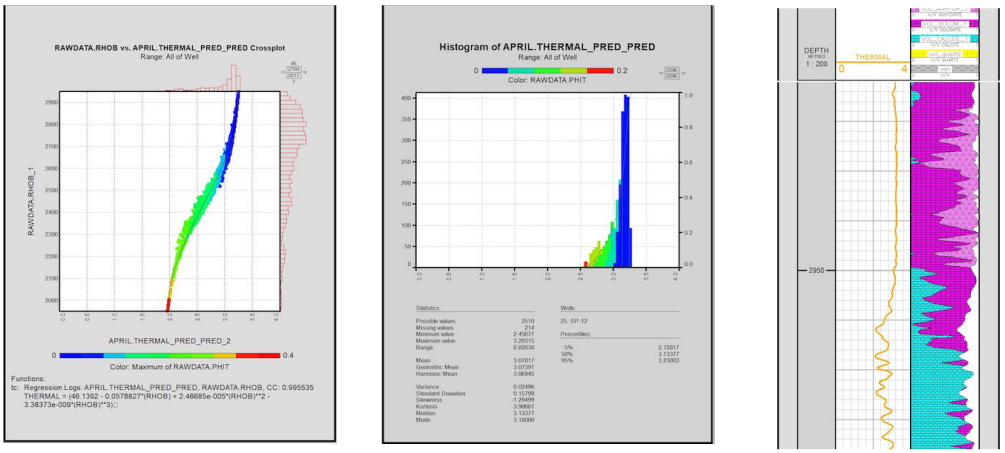

Figure 4.16: (a)Cross-plot of TC predicted and Density log colored by total porosity,(b)Histogram of TC colored by total porosity, (c) TC curve and lithology track (well-1, Third oil field)

First Oil Field	Well	MAE	MSE	R-squared
	1	0.03	0	0.987
	2	0.04	0	0.97

Figure 4.17: Table of Performance Metrics for the first Oil Field: MAE, MSE, and R-squared

analysis, are essential to confirm the geothermal potential and optimize the system design.

4.3 EVALUATING PREDICTIVE MODEL(ANN) USING MAE,MSE R-SQUARED

The following data represent the performance metrics of an Artificial Neural Network (ANN) model for thermal prediction across three different oil fields. The metrics used are Mean Absolute Error (MAE), Mean Squared Error (MSE), and R-squared (R^2). These metrics provide insights into the accuracy and reliability of the model's predictions for each well in the respective oil fields.

4.3.1 FIRST OIL FIELD

Figure4.17 shows the ANN Model Performance for well 1 and well 2.

Well-1: The ANN model accurately predicts thermal properties with a low Mean Absolute Error (MAE) of 0.032 and Mean Squared Error (MSE) of 0.002. The R-squared value of 0.987 shows that 98.7% of the variance in the data is explained by the model, indicating an excellent fit.

Well-2: Although Well 2 shows slightly higher MAE (0.040) and MSE (0.003) compared to Well 1, the model still performs well. The R-squared value of 0.970 suggests that the model explains 97% of the variance.

4.3.2 SECOND OIL FIELD

Figure4.18 shows the ANN Model Performance for wells 1 to 6.

Well 1: Higher MAE (0.093) and MSE (0.078) indicate less precise predictions compared to Oil Field 1. However, an R-squared value of 0.920 still shows that the model explains 92% of the variance, indicating a strong model fit.

Well 2: This well has the highest MAE (0.259) and MSE (0.081) in Oil Field 2, suggesting more significant prediction errors. While lower, the R-squared value of 0.810 still shows reasonable model performance.

Well 3: With an MAE of 0.166 and MSE of 0.048, the model performs better than Well 2 but not as well as for the other wells. The R-squared value of 0.890 indicates a good fit.

Well 4: The best performance in Oil Field 2, with a low MAE (0.039) and MSE (0.008), and an excellent R-squared value of 0.960, indicating high predictive accuracy.

Well 5: Moderate MAE (0.107) and high MSE (0.080) with an R-squared value of 0.900, indicating good performance but with some significant errors.

Well 6: This well also shows strong performance with an MAE of 0.086 and MSE of 0.013. An R-squared value of 0.930 indicates a high degree of variance, as the model explains.

	Well	MAE	MSE	R-squared
Second Oil Field	1	0.09	0.08	0.92
	2	0.26	0.08	0.81
	3	0.17	0.05	0.89
	4	0.04	0.01	0.96
	5	0.11	0.08	0.90
	6	0.09	0.01	0.93

Figure 4.18: Table Performance Metrics for the Second Oil Field: MAE, MSE, and R-squared

	Well	MAE	MSE	R-squared
Third Oil Field	1	0.03	0	0.99
	2	0.03	0	0.988

Figure 4.19: Table of Performance Metrics for the third Oil Field: MAE, MSE, and R-squared

4.3.3 Third oil field

In Figure4.19, performance metrics for wells 1 and 2 are shown for the ANN model.

Well 1: The ANN model achieves excellent performance with a very low MAE of 0.029 and MSE of 0.001. The R-squared value of 0.990 indicates that the model explains 99% of the variance, demonstrating an almost perfect fit.

Well 2: Similarly, this well shows a very low MAE of 0.028 and MSE of 0.001, with an R-squared value of 0.98, confirming the model's high accuracy and reliability.

5

Discussion and conclusion

5.1 CONCLUSION

This chapter discusses the findings from applying neural networks to predict ground thermal properties using well-log datasets. I analyze the results from various wells and oil fields to understand the model's performance and the underlying patterns in the data. This chapter concludes with an assessment of the implications of these findings and potential research directions.

In recent years, there has been a global shift towards renewable energy due to the negative environmental impacts of fossil fuels, such as greenhouse gas emissions, and the high costs and volatility associated with oil and gas. Climate change concerns have driven many countries to invest in renewable energy sources like wind farms, solar power, and geothermal energy. Geothermal energy has gained significant interest because it provides a constant energy source as the heat from the Earth's interior is always available, unlike solar and wind energy. This reliability makes geothermal energy particularly attractive for direct heating and cooling systems applications.

Many existing oil and gas wells offer a unique opportunity to be converted into geothermal wells, which can significantly reduce costs and risks associated with drilling new wells and save time. Utilizing well-log data from these wells can provide valuable insights into ground thermal properties without the high expenses related to coring and core analysis. Well-log data is more readily available and less expensive compared to core samples.

Well-log data can be analyzed using various methods to determine ground thermal properties. This study specifically focuses on using artificial neural networks (ANN) due to their higher accuracy and more intelligent data classification compared to regression methods. Each data set is trained using the ANN method, which determines the best relationship between the training data set. For validation, the N-fold method is used, where 25% of the data is utilized to estimate the model, and the results are then propagated to the remaining 75% of the data. Comparing the two models helps ensure the reliability of the ANN model.

Using ANN, we can accurately determine thermal conductivity from well-log data, which is crucial for studying geothermal potential. Other properties such as porosity, permeability, water saturation, and mineral composition can also be derived from well-log data. This method saves significant time and costs. For instance, analyzing ten wells through coring would require much more time and expense than using well-log data with ANN.

This study concludes with the realization that ANN-based analysis of well-log data is a powerful, efficient, and cost-effective method for exploring geothermal energy potential, providing a solid foundation for future research and practical applications in the renewable energy sector.

In the first oil field, which has a heterogeneous formation comprising five different lithologies (anhydrite, dolomite, limestone, sandstone, and shale), the mean value

of geothermal conductivity is estimated to be 2.7 $W/m \cdot K$ using artificial neural networks. Considering the temperature of 115 degrees Celsius at a depth of 3800 meters and the water saturation, this oil field can be regarded as a significant target for medium geothermal system applications. Fluid content is the main factor that can affect thermal conductivity in this oil field because oil is present in the sandstone zone.

In the second oil field, the thermal conductivity is estimated using Artificial Neural Network (ANN) prediction and has a mean value of about 2.8. The lithology of the formation is limestone and is considered homogeneous. The temperature at a depth of 4200 meters is approximately 137 degrees, and the water saturation is lower than the first oil field. This formation is potentially suitable for medium to high geothermal system applications. It is important to note that porosity is the main parameter influencing thermal conductivity in this formation.

In the last oil field, thermal conductivity is also predicted using the ANN method, yielding a value of about 2.9. The temperature in this field ranges from 85 to 105 degrees, making it suitable for shallow geothermal system applications. The thermal conductivity in this field is influenced by mineral composition, porosity, and fluid content.

The performance of the ANN model varies across the three oil fields, demonstrating its adaptability and robustness in predicting thermal properties. In Oil Field 1, both wells consistently exhibit high performance, with excellent R-squared values indicating a strong model fit. Oil Field 2 shows more variability in performance, with Well 2 displaying the least accuracy. However, most wells in this field still demonstrate good to excellent R-squared values, highlighting the model's general reliability. Oil Field 3 has exceptional performance in both wells, with very low errors and near-perfect R-squared values. These results collectively emphasize the ANN model's capability to deliver high accuracy and strong explanatory power across different wells and oil fields, proving its robustness in thermal property prediction.

Further studies are needed to assess the geothermal potential of these fields fully. These studies should include permeability testing to determine fluid flow capacity, assessing the feasibility of hydraulic fracturing to improve permeability, and detailed geological and geophysical surveys to map subsurface structures. It is also important to measure thermal gradients to understand temperature distribution with depth and to create detailed reservoir models to predict system behavior. Additionally, an economic feasibility analysis and environmental impact assessments are necessary to evaluate the cost-effectiveness and potential return on investment and to identify and mitigate potential risks. Water chemistry analysis can help determine potential impacts on the geothermal system and surface facilities, and implementing seismic monitoring can help detect induced seismicity. These thorough studies will provide a better understanding of the geothermal potential and will assist in optimizing the design and implementation of the geothermal system in the oil field.

5.2 SUGGESTIONS

By utilizing this study's findings, researchers can improve the simulation of the geothermal gradient and reservoir behavior, leading to a more precise design and implementation of the geothermal system in the oil field.

In the future, long-term thermal monitoring should be prioritized to continuously monitor changes in temperature and thermal gradients, ensuring data accuracy over an extended period of time. Developing dynamic reservoir models is crucial, as more advanced models will improve predictive capabilities and optimize reservoir behavior under various conditions. To inform sustainable and cost-effective development strategies, comprehensive studies on geothermal projects' economic and environmental feasibility are required to assess their viability, potential returns, and environmental impacts.

Other methods, such as fuzzy logic and clustering data, could also be explored to predict thermal conductivity. They could be compared with the ANN method, as these approaches might offer different advantages in handling uncertainties and identifying patterns in complex datasets.

References

[1] Thomas J Ahrens. *Rock physics and phase relations: a handbook of physical constants*. American geophysical union, 1995.

[2] Juliana Aparecida Anochi, Reynier Hernández Torres, and Haroldo Fraga de Campos Velho. "Two geoscience applications by optimal neural network architecture". In: *Pure and Applied Geophysics* 177.6 (2020), pp. 2663–2683.

[3] Rahman Ashena. "Analysis of some case studies and a recommended idea for geothermal energy production from retrofitted abandoned oil and gas wells". In: *Geothermics* 108 (2023), p. 102634.

[4] Ali Bassam et al. "Estimation of static formation temperatures in geothermal wells by using an artificial neural network approach". In: *Computers & Geosciences* 36.9 (2010), pp. 1191–1199.

[5] Maria Estefania Santamaria Cerrutti. "Geothermal Energy". In: (2020).

[6] Christoph Clauser, Ernst Huenges, et al. "Thermal conductivity of rocks and minerals". In: *Rock physics and phase relations: a handbook of physical constants* 3 (1995), pp. 105–126.

[7] Giorgia Dalla Santa et al. "An updated ground thermal properties database for GSHP applications". In: *Geothermics* 85 (2020), p. 101758.

[8] Adelina P Davis and Efstathios E Michaelides. "Geothermal power production from abandoned oil wells". In: *Energy* 34.7 (2009), pp. 866–872.

[9] Mary H Dickson and Mario Fanelli. *Geothermal energy: utilization and technology*. Routledge, 2013.

[10] AD Dongare, RR Kharde, Amit D Kachare, et al. "Introduction to artificial neural network". In: *International Journal of Engineering and Innovative Technology (IJEIT)* 2.1 (2012), pp. 189–194.

[11] F Farshad, James D Garber, and Juliet N Lorde. "Predicting temperature profiles in producing oil wells using artificial neural networks". In: *SPE Latin America and Caribbean Petroleum Engineering Conference*. SPE. 1999, SPE–53738.

[12] Sven Fuchs and Andrea Förster. "Well-log based prediction of thermal conductivity of sedimentary successions: a case study from the North German Basin". In: *Geophysical Journal International* 196.1 (2014), pp. 291–311.

[13] Jianwen Gan et al. "Underground Garage Patrol Based on Road Marking Recognition by Keras and Tensorflow". In: *Applied Sciences* 13.4 (2023), p. 2385.

[14] Bruno Goutorbe, Francis Lucazeau, and Alain Bonneville. "Using neural networks to predict thermal conductivity from geophysical well logs". In: *Geophysical Journal International* 166.1 (2006), pp. 115–125.

[15] Daniel P Hampson, James S Schuelke, and John A Quirein. "Use of multiattribute transforms to predict log properties from seismic data". In: *Geophysics* 66.1 (2001), pp. 220–236.

[16] Andreas Hartmann, Volker Rath, and Christoph Clauser. "Thermal conductivity from core and well log data". In: *International Journal of Rock Mechanics and Mining Sciences* 42.7-8 (2005), pp. 1042–1055.

[17] Valentin Heusgen. "Geothermal Energy". In: (2019).

[18] Umid Kakemem et al. “Sedimentology and sequence stratigraphy of automated hydraulic flow units–The Permian Upper Dalan Formation, Persian Gulf”. In: *Marine and Petroleum Geology* 147 (2023), p. 105965.

[19] Soteris A Kalogirou. “Applications of artificial neural-networks for energy systems”. In: *Applied energy* 67.1-2 (2000), pp. 17–35.

[20] Anuj Karpatne et al. “Theory-guided data science: A new paradigm for scientific discovery from data”. In: *IEEE Transactions on knowledge and data engineering* 29.10 (2017), pp. 2318–2331.

[21] Hossein Kheirollahi, Navid Shad Manaman, and Ahsan Leisi. “Robust estimation of shear wave velocity in a carbonate oil reservoir from conventional well logging data using machine learning algorithms”. In: *Journal of Applied Geophysics* 211 (2023), p. 104971.

[22] Maher Nasr et al. “Geothermal potential of the St. Lawrence Lowlands sedimentary basin from well log analysis”. In: *Geothermics* 75 (2018), pp. 68–80.

[23] Sina Rashidi et al. “Shear modulus prediction of embedded pressurized salt layers and pinpointing zones at risk of casing collapse in oil and gas wells”. In: *Journal of Applied Geophysics* 183 (2020), p. 104205.

[24] Luisa Rolon et al. “Using artificial neural networks to generate synthetic well logs”. In: *Journal of Natural Gas Science and Engineering* 1.4-5 (2009), pp. 118–133.

[25] Mehdi Safari. “Effect of Different Water Injection Rate on Reservoir Performance: A Case Study of Azadegan Fractured Oil Reservoir”. In: *Proceedings of the International Conference of Oil, Gas, Petrochemical and Power Plant, Tehran, Iran*. Vol. 1. 2012, p. 8.

[26] Amer A Shehata, Osama A Osman, and Bassem S Nabawy. “Neural network application to petrophysical and lithofacies analysis based on multiscale data: an integrated study using conventional well log, core and borehole image data”. In: *Journal of natural gas science and engineering* 93 (2021), p. 104015.

[27] Donald A Singer and Ryoichi Kouda. “Use of a neural network to integrate geoscience information in the classification of mineral deposits and occurrences”. In: *Proceedings of exploration*. Vol. 97. 1997, pp. 127–134.

[28] Jian Sun et al. “Optimization of models for a rapid identification of lithology while drilling-A win-win strategy based on machine learning”. In: *Journal of Petroleum Science and Engineering* 176 (2019), pp. 321–341.

[29] Somayeh Tabasi et al. “Optimized machine learning models for natural fractures prediction using conventional well logs”. In: *Fuel* 326 (2022), p. 124952.

[30] Jefferson W Tester et al. “The future of geothermal energy”. In: *Massachusetts Institute of Technology* 358 (2006), pp. 1–3.

[31] Bernard P Tissot and Dietrich H Welte. *Petroleum formation and occurrence*. Springer Science & Business Media, 2013.

[32] Jun Wang et al. “Missing well logs prediction using deep learning integrated neural network with the self-attention mechanism”. In: *Energy* 261 (2022), p. 125270.

[33] Yu-chen Wu and Jun-wen Feng. “Development and application of artificial neural network”. In: *Wireless Personal Communications* 102 (2018), pp. 1645–1656.

[34] Ahmed Ali Zerrouki et al. “A Preliminary study of relationships between thermal conductivity and petrophysical parameters in Hamra Quartzites reservoir, Hassi Messaoud field (Algeria)”. In: *Journal of African Earth Sciences* 151 (2019), pp. 461–471.

Acknowledgments

In completion of my thesis, I would like to express my deepest gratitude to my supervisor, Professor Antonio Galgaro, for his guidance, expertise, and unwavering support. His mentorship has helped me overcome challenges and shape my research.

Additionally, I would like to express my gratitude to my wife, Paria, for her constant encouragement, love, and support throughout the process. I have found true strength in her unwavering support and understanding.

Moreover, I would like to thank my family and friends, especially my parents, for their unwavering support and for allowing me to focus on my studies. I have been inspired by their constant support and interest in my work.